Electronic Supporting Information for

The carbon nanotube formation parameter space: Data mining and mechanistic understanding for efficient resource use

Wenbo Shi[a], Ke Xue[b], Eric R. Meshot[c], Desiree L. Plata[a*]
[a]Department of Chemical and Environmental Engineering, Yale University, New Haven, CT, United States
[b]Department of Civil and Environmental Engineering, Duke University, Durham, NC, United States
[c]Physical and Life Sciences Directorate, Lawrence Livermore National Laboratory, Livermore, CA, United States

*Corresponding author: desiree.plata@yale.edu; phone: 203-496-3066

Table of Content

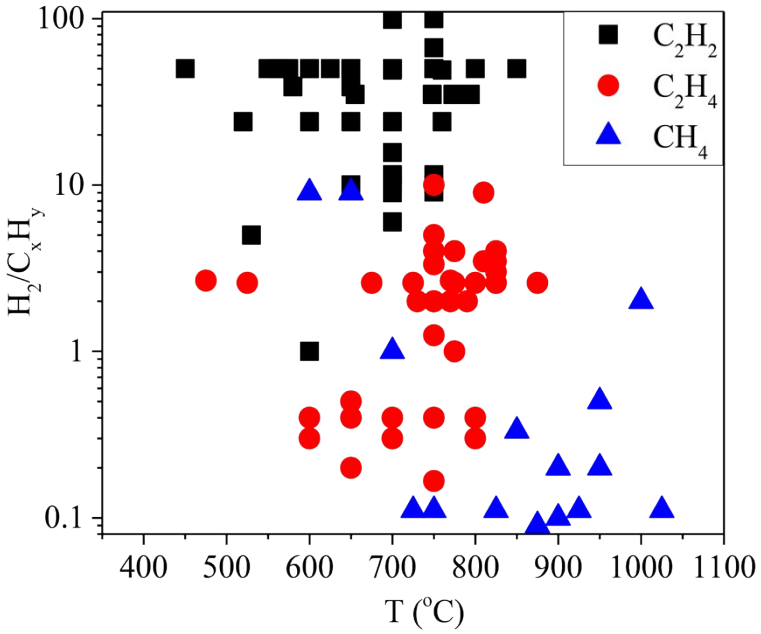

Fig. S1 Temperature and H_2/C_xH_y ratio utilized for CH_4, C_2H_4, and C_2H_2 in the literature-based CNT growth parameter investigation. Note that, due to incapability of presenting $H_2/C_xH_y=0$ data points in this logarithmic scale and some reports using alternative moderating or influencing gas (*e.g.*, NH_3) rather than H_2, the number of data point in this map is less than that in the statistical distribution of each individual parameter (*i.e.*, number of data point in this figure is less than in Fig.2 and Fig.5 in the main text).

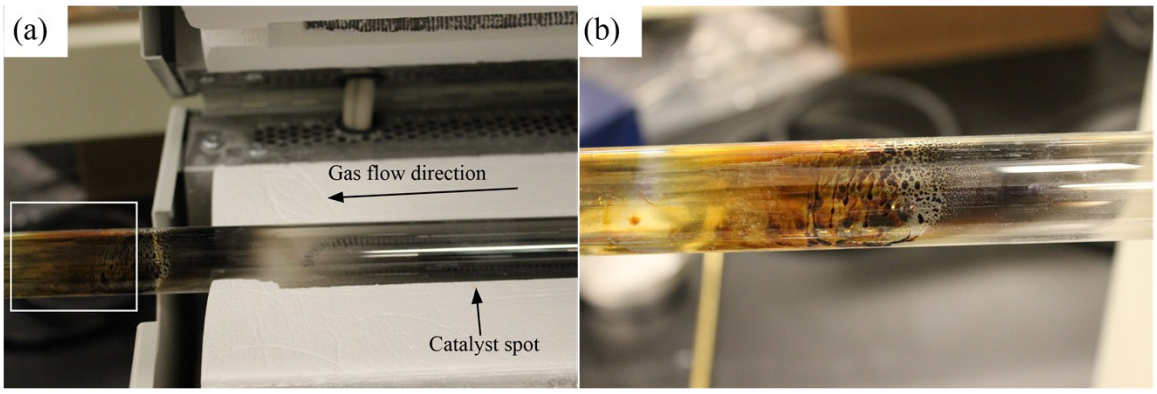

Fig. S2 Severe side-reactions happened under 10% C_2H_2 (*i.e.*, 50 sccm C_2H_2 in total 500 sccm flow rate) at 800 ^oC. Photograph of the byproducts residual inside the quartz tubing after CNT growth (a) and zoomed-in photograph of the selected area in (a) exhibited obvious yellow-color indicative of oily byproducts (b).

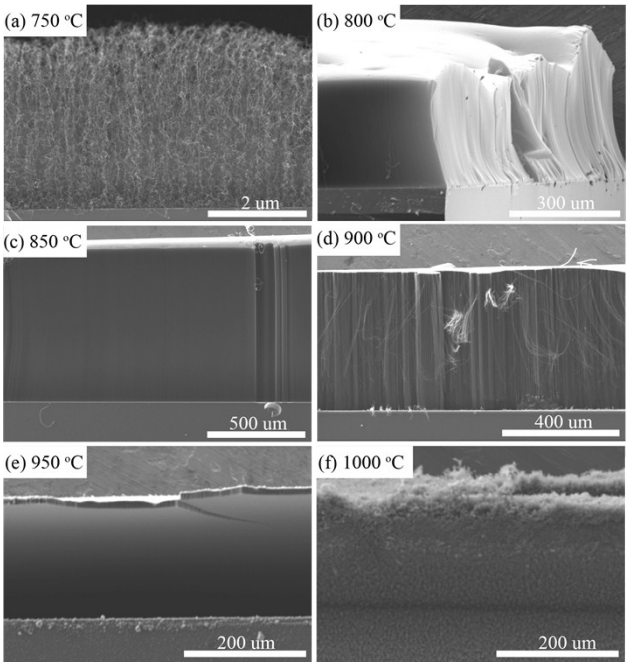

Fig. S3 SEM images demonstrated the morphology evolution of the products temperature at 10% C_2H_4 gas recipe on Fe-Al_2O_3 substrate catalyst. Micrometer-scale CNT forests were yielded at 750 °C (a), followed by hundreds-um-scale CNT forests at 800 °C (b), 850 °C (c), 900 °C (d). In contrast, products shifted to other carbon materials at 950 °C (e) and 1000 °C (f).

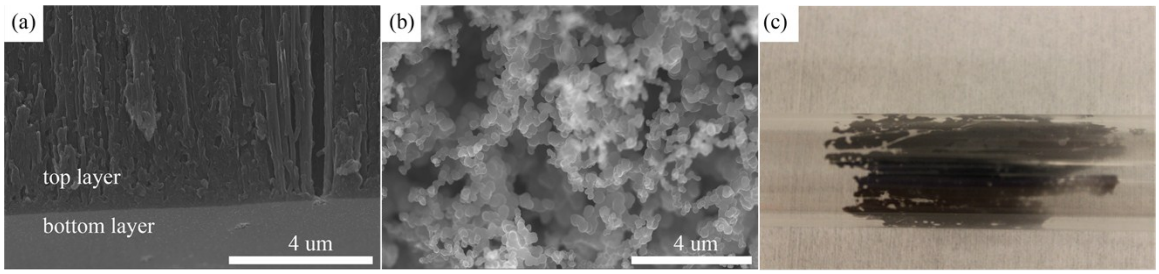

Fig. S4 Non-CNT products yielded at 950 ^{o}C (a) and 1000 ^{o}C (b and c) with 10% C_2H_4 gas composition (*i.e.*, 50 sccm C_2H_4 diluted by Ar). At 950 ^{o}C, the top layer was a bundle-like structure and the bottom layer was made up of cheese-like carbonaceous products, indicating that CNT was grown first then shifted to non-crystalline carbon materials deposition (a) when catalysts were fully deactivated after going through tough thermal treatment. SEM image of 1000 ^{o}C growth showed that the products were nanospheres of several hundred nm approximate diameters (b). Those carbon nanospheres were extremely sticky to the quartz tubing inner-wall and even air-baking (500 sccm air, 850 ^{o}C, 1 h) and acetone-wash could not remove them, as presented in (c).

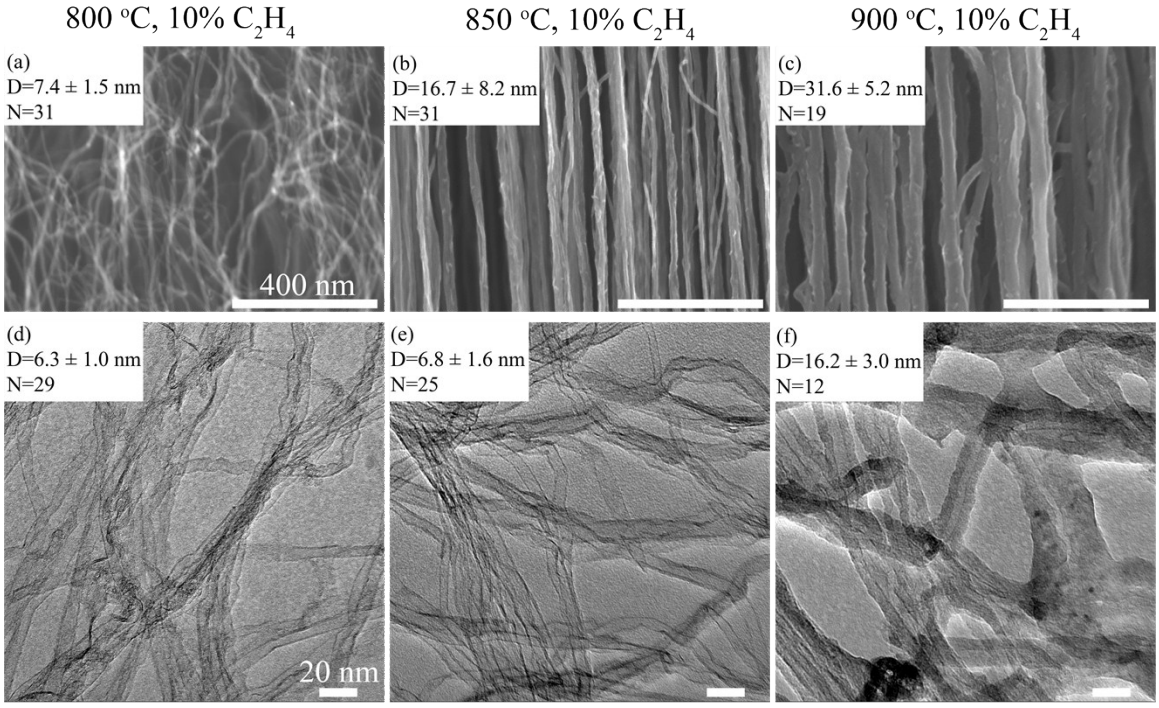

Fig. S5 Comparison of the average CNT bundle diameter measured from high resolution SEM images and average individual CNT diameter measured from the TEM images of the CNT samples grown from 10% C_2H_4 at 800 °C (a and d), 850 °C (b and e) and 900 °C (c and f). Average diameter (denoted as D) was labeled in each image based on the counting of N tubes.

The significant difference of the nano-scale morphology of the CNT bundles at different temperatures suggests more severe gas phase pyrolysis at higher temperature[1]. At 800 °C, CNTs tend to be in individual tube form and wrapped loosely together and less aligned. However, at 850 °C, CNTs wrapped tightly and generated well-aligned CNT bundles. The 900 °C trial yielded an even wider diameter bundles. Tubes formed at 800 °C and 850 °C were both few-walled CNTs, while 900 °C wall numbers increased sharply and gave multi-walled CNTs (MWCNTs). Comparing the tube diameters measured in SEM and TEM images, we found that at 800 °C, tube diameters in SEM images were approximately equal to the tube diameters in TEM images, while at 850 and 900 °C, tube diameters in SEM images were about 2 times the tube diameters in TEM images, indicating the aggregation of few individual tubes to form bundles.

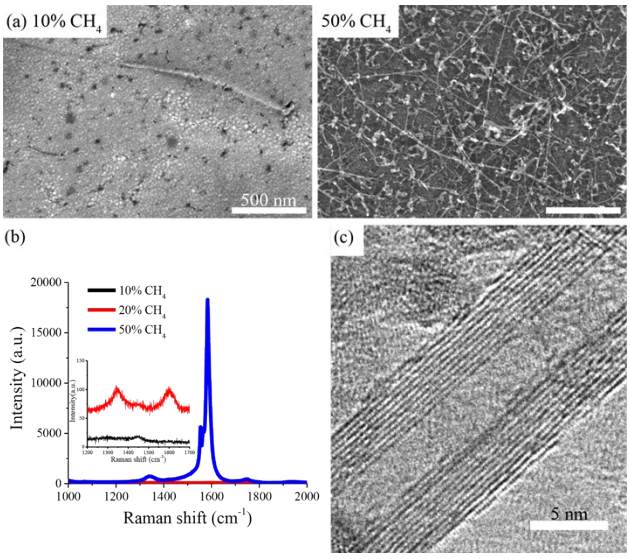

Fig. S6 Increased CH_4 concentration escalated CNT production at 950 ^oC on Fe-Al_2O_3 substrate catalyst. Comparison of the SEM images of the at 10% CH_4 and 50 % CH_4 (a) and Raman spectra intensification along with CH_4 concentration (b) of the substrate surface both indicated this yield increase. High Resolution TEM (HR-TEM) image (c) of the 50% CH_4 confirmed the presence of MWCNTs.

The increased CNT yield can be revealed from the escalated intensity of Raman spectra. Along with the increase of CH_4 concentration, the substrate grown from 20% CH_4 exhibited a weak, defect-derived D-band (approximately 1350 cm^{-1}) and graphite-derived G-band (approximately 1600 cm^{-1}), whereas at 50% CH_4, the D and G band intensity suddenly ascended (b). The high G/D ratio at 50% CH_4 implied considerable amount of graphitic structure in the as-grown products. The crystalline graphitic nanostructures were proved to be MWCNTs through HR-TEM (d).

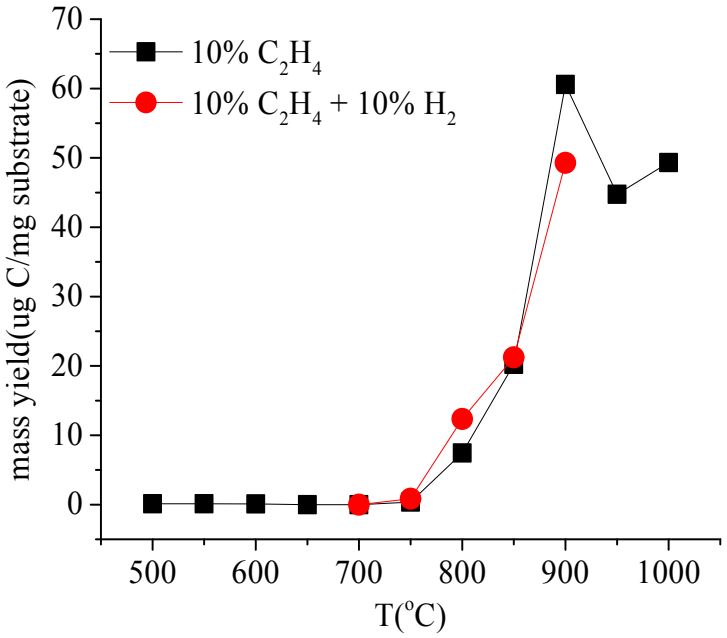

Fig. S7 Comparison of the mass yield of CNT growth from 10% C_2H_4 with and without 10% H_2. At 850 to 900 °C, adding H_2 either yield equal mass or less mass but higher forest height, indicating less density CNT products.

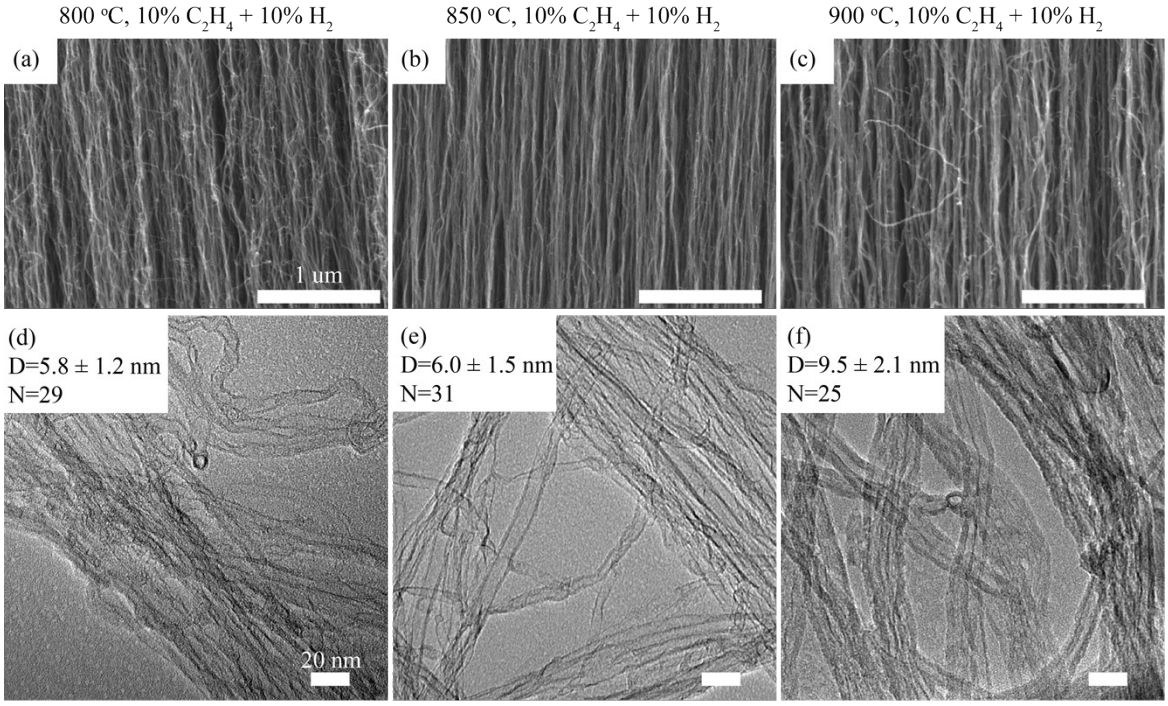

Fig. S8 Comparison of the CNT bundle morphology in high resolution SEM images and average individual CNT diameter measured from the TEM images of the CNT samples grown from 10% C_2H_4 and 10% H_2 at 800 °C (a and d), 850 °C (b and e) and 900 °C (c and f). SEM images didn't show severe bundle aggregation. Average diameter (denoted as D) was labeled in each image based on the counting of N.

Calculation of thermal energy input during CNT growth

Specific heat of the tube furnace insulation material: Cp=1.13 J/(g×K)

Mass density of the tube furnace insulation material: ρ=210000 g/m^3

Wall thickness: w=0.127 m

Ambient temperature To=25 °C

Thermal heat requirement to ramping to Ti

$$Q1 = Cp \times \rho \times w \times \frac{Ti - To}{2}$$

Thermal conductivity λ=0.17 W/(m*K)

Heat loss at Ti for t=15 min

$$Q2 = \lambda \times \frac{Ti - To}{w} * t$$

For the heating surface area (cylinder shape with D=0.0254 m, L=0.3048 m)

$$A = \pi \times D \times L$$

Then, the total energy input (Note that no recycling of heat via heat exchangers is included in the calculation):

$$J = (Q1 + Q2) \times A$$

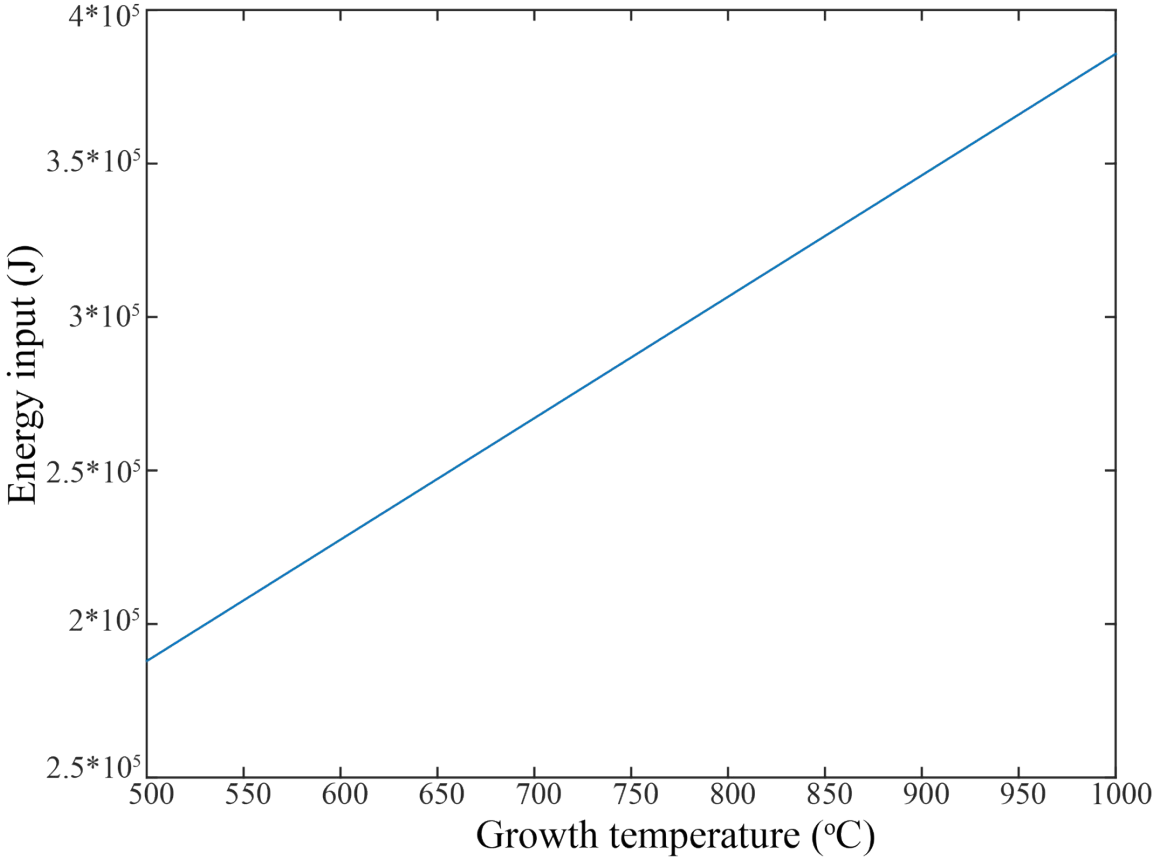

Fig. S9 Energy input requirement for single CNT growth process at different temperatures ranging from 500 °C to 1000 °C

Assumptions:

(1) the temperature deference is from 700 °C to 800 °C

(2) each growth experiment yield 0.3 mg CNT
(3) production capacity of CNT is 2.2×10^6 kg[2]

Then, energy savings (SJ) are calculated as:

$$SJ = \frac{J(800) - J(700)}{0.3 \times 10^6} \times 2.2 \times 10^6$$

Based on the data from US Department of Energy, the annual electricity consumption for a US household was 10812 kWh in 2015.[3] The equivalent number of household electricity consumption from this saved energy, N, is given by:

$$N = \frac{SJ}{10812 \times 3.6 \times 10^6}$$

References

1. X. Y. Lin, W. Zhao, W. B. Zhou, P. Liu, S. Luo, H. M. Wei, G. Z. Yang, J. H. Yang, J. Cui, R. C. Yu, L. N. Zhang, J. P. Wang, Q. Q. Li, W. Y. Zhou, W. S. Zhao, S. S. Fan and K. L. Jiang, *ACS Nano*, 2017, **11**, 1257-1263.
2. M. F. L. De Volder, S. H. Tawfick, R. H. Baughman and A. J. Hart, *Science*, 2013, **339**, 535-539.
3. U. S. Department of Energy, How much electricity does an American home use?, https://www.eia.gov/tools/faqs/faq.cfm?id=97&t=3, (accessed Dec, 2016).

Group	Paper #	annea l time	anneal gas	C_xH_y flow	H_2 flow	H_2/ C_xH_y	carrier gas	carrier gas flow	growth enhancer (Y/N)	Growth enhancer	catalyst	Tem.	reactor	growth time	terminal length	yield	SWCNT or MWCNT
										CH_4							
Zhang& Wei	8	25 min at 900 °C	H_2:Ar=2:1 in volume with a total flow of 200 sccm	1/3×75 sccm	2/3×75 sccm	2.00	no	no	yes	0.43% H_2O	an ethanol solution of $FeCl_3$ (0.03 mol/L) coated on the substrates. Substrate is 500 nm SiO_2 on single crystal silicon wafer	1000 °C	Tube furnace, length: 1.5 m; outer/inner diameter: 35 mm/31 mm	15 min			Graphene/SW CNT
Zhang& Wei	12	ramping to 1000 °C	400 mL/min	400 mL/min	no	0.00	Ar	400 mL/min	no	no	FeMgAl layered double hydroxides	1000 °C	horizontal quartz tube furnance	2, 5, 15, 30, 60 min			short aligned SWCNT
Ajayan	5										Pd particles on SiO_2	1000 °C	hot wall CVD				SWCNT strands
Hart	2			360 sccm	40 sccm	0.11			no	no	1.5 nm Fe+ 3 nm Mo + 20 nm Al_2O_3	1025 °C	single-zone atmospheric pressure quartz tube furnace with inside diameter of 22 mm and a 30 scm long heating zone				
Homma	19	10 min at 900 °C	air	300 sccm at 6-7×10^4 Pa	no	0.00	no	no	no	no	Au-Si nanoparticle	1100 °C	hot wall furance				
Roberton	38	5 min at 600 °C		5 sccm CH_4	45 sccm	9.00	no	no	no	no	0.5 nm Al_2O_3 +0.3-0.5nm Fe+ 5 nm Al_2O_3	600 °C	remote plasma CVD method				DWCNT
Roberton	38	5 min at 640 °C		5 sccm CH_4	45 sccm	9.00	no	no	no	no	0.5 nm Al_2O_3 +0.3-0.5nm Fe+ 5 nm Al_2O_3	600 °C	remote plasma CVD method				
Zhang& Wei	29	5 min at 600 °C	hydrogen plasma	20 sccm	180 sccm	9.00	no	no	no	no	patterned Fe catalyst layer on Aluminum	600 °C	2.45 GHz microwave CVD	1 h	540 um		MWCNT
Zhang & Wei	37	20 min	hydrogen plasma	20 sccm	180 sccm	9.00	no	no	no	no	2 nm Fe+2 nm Al+500 nm Ni + TiN	600 °C	microwave plasma CVD				MWCNT
Zhang & Wei	38			20 sccm	180 sccm	9.00	no	no	no	no	2 nm Fe+2nm Al+150 nm Ni	600 °C	microwave plasma CVD				
Roberton	35	5 min	20 sccm CH_4+180 sccm H_2	20 sccm CH_4	180 sccm	9.00	no	no	no	no	0.5 nm Al+0.5-0.7 nm Fe+10 nm Al_2O_3	650 °C	microwave plasma-enhanced chemical vapor deposition	10 min	200 um		SWCNT
Roberton	35	5 min	20 sccm CH_4+180 sccm H_2	20 sccm CH_4	180 sccm	9.00	no	no	yes	20 sccm H_2O via a needle-valve-controlled inlet	0.5 nm Al+0.5-0.7 nm Fe+10 nm Al_2O_3	650 °C	cold wall				
Homma	7			50 sccm	50 sccm	1.00	no	no	no	no	Fe on SiO_2 pillar-patterned substrates	700 °C	hot filament CVD	5 min			SWCNT
Hart	2			360 sccm	40 sccm	0.11			no	no	1.5 nm Fe+ 3 nm Mo + 20 nm Al_2O_3	725 °C	single-zone atmospheric pressure quartz tube furnace with inside diameter of 22 mm and a 30 scm long heating zone				
Hart	2			360 sccm	40 sccm	0.11			no	no	1.5 nm Fe+ 3 nm Mo + 20 nm Al_2O_3	750 °C	single-zone atmospheric pressure quartz tube furnace with inside diameter of 22 mm and a 30 scm long heating zone				
Homma	2			300 sccm at 100-500 Torr	sno	0.00	no	no	no	no	Fe_2O_3, Fe and Ni nanoparticles on SiO_2	750 °C	furnace for CVD experiments consisted of a quartz tube with a carbon heater mounted inside a stainless steel chamber. The sample(10 mm×10 mm or smaller) was placed on a carbon plate (80 mm-diam.) above the heater				SWCNT

Group	Paper #	annea l time	anneal gas	C_xH_y flow	H_2 flow	H_2/ C_xH_y	carrier gas	carrier gas flow	growth enhancer (Y/N)	Growth enhancer	catalyst	Tem.	reactor	growth time	terminal length	yield	SWCNT or MWCNT
Homma	3			300 sccm at 67 kPa	no	0.00	no	no	no	no	Fe and Co with a mean particle size of 30 nm or Fe_2O_3 with a mean size of 10 nm on SiO_2 , or 0.5 and 5 nm thin film catalyst	750 °C for plotting 750 °C to 800 °C	furnace for CVD experiments consisted of a quartz tube with a carbon heater mounted inside a stainless steel chamber. The sample (10 mm×10 mm or smaller) was placed on a carbon plate (80 mm-diam.) above the heater				
Homma	1			300 sccm at 200 Torr	no	0.00	no	no	no	no	Co thin fim on Si pillar	800 °C	furnace for CVD experiments consisted of a quartz tube with a carbon heater mounted inside a stainless steel chamber				
Homma	4			300 sccm at 500 Torr	no	0.00	no	no	no	no	Fe or Co thin films (0.5 to 1 nm) on SiO_2	800 °C	substrates were placed on the carbon plate inside a quartz tube above the heater in the CVD furnace				
Homma	3			300 sccm at 67 kPa	no	0.00	no	no	no	no	Fe and Co with a mean particle size of 30 nm or Fe_2O_3 with a mean size of 10 nm on SiO_2 , or 0.5 and 5 nm thin film catalyst	800 °C	furnace for CVD experiments consisted of a quartz tube with a carbon heater mounted inside a stainless steel chamber. The sample (10 mm×10 mm or smaller) was placed on a carbon plate (80 mm-diam.) above the heater				
Hart	2			360 sccm	40 sccm	0.11			no	no	1.5 nm Fe+ 3 nm Mo + 20 nm Al_2O_3	825 °C	single-zone atmospheric pressure quartz tube furnace with inside diameter of 22 mm and a 30 scm long heating zone				
Roberton	46	10 min at 850 °C	200 mbar H_2	3/4×200 mbar	1/4×200 mbar	0.33	no	no	no	no	1 nm Ni+8 nm Al	850 °C	low pressure chemical vapor deposition (cold wall)				SWCNT
Roberton	47	10 min	H_2 at 200 mbar	3/4×200 mbar	1/4×200 mbar	0.33	no	no	no	no	Bimetallic catalyst films (1nm Ni over 8 nm Al) on Si	850 °C	low pressure chemical vapor deposition (cold wall)				
Hart	2				H_2/CH_4 ratio not mention						Mo/Fe/Al_2O_3	875 °C	single-zone atmospheric pressure quartz tube furnace with inside diameter of 22 mm and a 30 scm long heating zone				
Hart	2				H_2/CH_4 ratio not mention						Fe/Al_2O_3	875 °C	single-zone atmospheric pressure quartz tube furnace with inside diameter of 22 mm and a 30 scm long heating zone				
Hart	2					0.09					1.5 nm Fe+ 3 nm Mo + 20 nm Al_2O_3	875 °C	single-zone atmospheric pressure quartz tube furnace with inside diameter of 22 mm and a 30 scm long heating zone				
Roberton	12	10 min	200 sccm H_2	500 sccm CH_4	100 sccm	0.20	no	no	no	no	0.1-0.2 nm or 0.7 nm-1.0 nm Ta-oxide/SiO_2	900 °C	hot wall reactor				
Roberton	47	10 min	200 sccm H_2	500 sccm CH_4	100 sccm	0.20	no	no	no	no	0.1 nm Fe on SiO_2	900 °C	2 inch hot wall reactor				

Group	Paper #	annea l time	anneal gas	C_xH_y flow	H_2 flow	H_2/ C_xH_y	carrier gas	carrier gas flow	growth enhancer (Y/N)	Growth enhancer	catalyst	Tem.	reactor	growth time	terminal length	yield	SWCNT or MWCNT
Zhang & Wei	6	2.4 s	CH_4 at 0.6-1.3 m/s	total CH_4+Ar is 0.3 m/s		0.00	Ar				Fe/MgO catalyst with Fe loading of 1% (weight ratio)	900 °C	Downer-turbulent fluidized-bed reactor; Downer (1.5 m in length, 20 or 30 mm in diameter) and TFB (50 mm in diameter and 1 m in length)				
Zhang & Wei	12	ramping to 900 °C	400 mL/min	400 mL/min	no	0.00	Ar	400 mL/min	no	no	FeMgAl layered double hydroxides	900 °C	horizontal quartz tube furnance	10 min			Graphene/SW CNT
Zhang & Wei	13	5 min at 900 °C	50 mL/min H_2	500 mL/min	50 mL/min	0.10	no	no	no	no	FeMoMgAl layered double hydroxides (LDHs) films	900 °C	horizontal quartz tube furnance				
Zhang & Wei	35			80 mL/min	no	0.00	Ar	600 mL/min	no	no	Fe/MgO	900 °C	horizontal quart tube furnace (i.d. 35 mm, length 1200 mm)				
Hart	14	0-10 min	200 sccm H_2	500 sccm	100 sccm	0.20	no	no	no	no	ZrO_2	900 °C	three-zone Lindberg/Blue M furnace with a 62-cm heated length using 50-mm inner diameter fused quartz prºC ess tubes with a length of 138 cm	10 min			
Homma	2			300 sccm at 100-500 Torr	no	0.00	no	no	no	no	Fe_2O_3, Fe and Ni nanoparticles on SiO_2	900 °C	furnace for CVD experiments consisted of a quartz tube with a carbon heater mounted inside a stainless steel chamber. The sample(10 mm * 10 mm or smaller) was placed on a carbon plate (80 mm-diam.) above the heater				
Homma	4			300 sccm at 500 Torr	no	0.00	no	no	no	no	Fe or Co thin films (0.5 to 1 nm) on SiO_2	900 °C	substrates were placed on the carbon plate inside a quartz tube above the heater in the CVD furnace				
Homma	5			300 sccm	no	0.00	no	no	no	no	4 nm Fe_3O_4 nanoparticles on SiO_2 by spin-coating	900 °C	substrates were placed on the carbon plate inside a quartz tube above the heater in the CVD furnace				
Homma	8	5 min	300 sccm Ar	300 sccm at 500 Torr	no	0.00	no	no	no	no	0.05 or 5 mg/mL ferritin solutions (a protein shell encasing iron nanoparticles)	900 °C					
Homma	3			300 sccm at 67 kPa	no	0.00	no	no	no	no	Fe and Co with a mean particle size of 30 nm or Fe_2O_3 with a mean size of 10 nm on SiO_2 , or 0.5 and 5 nm thin film catalyst	900 °C for plotting 900 °C to 950 °C	furnace for CVD experiments consisted of a quartz tube with a carbon heater mounted inside a stainless steel chamber. The sample (10 mm×10 mm or smaller) was placed on a carbon plate (80 mm-diam.) above the heater	1-2 min			SWCNT
Homma	3			300 sccm at 67 kPa	no	0.00	no	no	no	no	Fe and Co with a mean particle size of 30 nm or Fe_2O_3 with a mean size of 10 nm on SiO_2 , or 0.5 and 5 nm thin film catalyst	950 °C for plotting 900 °C to 950 °C					
Hart	2			360 sccm	40 sccm	0.11			no	no	1.5 nm Fe+ 3 nm Mo + 20 nm Al_2O_3	925 °C	single-zone atmospheric pressure quartz tube furnace with inside diameter of 22 mm and a 30 scm long heating zone				
Roberton	12	10 min	200 sccm H_2	500 sccm CH_4	100 sccm	0.20	no	no	no	no	0.2 nm-1.0 nm Ta-oxide/Al_2O_3	950 °C	hot wall reactor				

Group	Paper #	annea l time	anneal gas	C_xH_y flow	H_2 flow	H_2/ C_xH_y	carrier gas	carrier gas flow	growth enhancer (Y/N)	Growth enhancer	catalyst	Tem.	reactor	growth time	terminal length	yield	SWCNT or MWCNT
Zhang & Wei	1	ramping to 950 °C with 20 °C /min	100 mL/min Ar	80 mL/min	no	0.00	Ar	20 mL/min	no	no	FeMgAl bifunctional layered double oxide catalysts	950 °C	TGA	15 min			
Zhang & Wei	1		Ar	0.05g CH_4/(gLDO×min)	no	0.00	no	no	no	no	FeMgAl bifunctional layered double oxide catalysts	950 °C	quartz fluidized bed with inner diameter of 50 mm and a height of 1500 mm, vertical electric tube furnace	90 s+ 810 s			
Zhang & Wei	1		Ar	0.15 gCH_4/(gLDO×min) in the first 90s, then 0.03 gCH_4/(gLDO×min) for another 810 s	no	0.00	no	no	no	no	FeMgAl bifunctional layered double oxide catalysts	950 °C	quartz fluidized bed with inner diameter of 50 mm and a height of 1500 mm, vertical electric tube furnace	30 min+30 min	10 um CNTs		nitrogen-doped aligned CNT/graphene
Zhang & Wei	4	ramping to 950 °C	500 mL/min Ar	400 mL/min	no	0.00	Ar	100 mL/min	no	no	FeMgAl LDH	950 °C	fluidized bed reactor; inner diameter of 20 mm and a height of 500 mm	30 min			Vine Tree CNTs
Zhang & Wei	5	ramping to 950 °C	100 mL/min Ar	100 mL/min	50 mL/min	0.50	Ar	100 mL/min	yes	Formamide (CH_3NO) in 0.1, 0.20, 0.50, 1.5, 3.0 mL/h	FeMoMgAl layered double hydroxides (LDHs)	950 °C	horizontal quartz tube furnance	3-6 min			SWCNT
Zhang & Wei	9	ramping to 950 °C	600 mL/min Ar	500 mL/min	no	0.00	Ar	100 mL/min	no	no	CoMgAl layered double hydroxides	950 °C	horizontal quartz tube furnance				
Zhang & Wei	12	ramping to 950 °C	400 mL/min	400 mL/min	no	0.00	Ar	400 mL/min	no	no	FeMgAl layered double hydroxides	950 °C	horizontal quartz tube furnance	10 min			Graphene/SWCNT
Homma	1			300 sccm at 500 Torr	no	0.00	no	no	no	no	Fe thin film on 100 nm diameter Si pillars	950 °C	furnace for CVD experiments consisted of a quartz tube with a carbon heater mounted inside a stainless steel chamber				
Homma	2			300 sccm at 100-500 Torr	no	0.00	no	no	no	no	Fe_2O_3, Fe and Ni nanoparticles on SiO_2	950 °C	furnace for CVD experiments consisted of a quartz tube with a carbon heater mounted inside a stainless steel chamber. The sample(10 mm×10 mm or smaller) was placed on a carbon plate (80 mm-diam.) above the heater				
Homma	4			300 sccm at 500 Torr	no	0.00	no	no	no	no	Fe or Co thin films (0.5 to 1 nm) on SiO_2	950 °C	substrates were placed on the carbon plate inside a quartz tube above the heater in the CVD furnace				
Zhang & Wei	32										Fe(Co/Ni)/Mo/MgO		nano-agglomerated fluidized-bed reactor	60 min			MWCNT
Hart	5	2 min	200 sccm H_2 + 200 sccm Ar	800 sccm	200 sccm	0.25	no	no	no	no	3.0 nm Mo + 1.5 nm Fe + 20 nm Al_2O_3		cold wall reactor, suspended silicon platform heater, 300 mm length, 48 mm internal diameter, 52 mm outer diameter	15 min			vertically aligned MWCNT
Hart	2								no	no	1.5 nm Fe+ 3 nm Mo + 20 nm Al_2O_3		single-zone atmospheric pressure quartz tube furnace with inside diameter of 22 mm and a 30 scm long heating zone				SWCNT

Group	Paper #	annea l time	anneal gas	C_xH_y flow	H_2 flow	H_2/ C_xH_y	carrier gas	carrier gas flow	growth enhancer (Y/N)	Growth enhancer	catalyst	Tem.	reactor	growth time	terminal length	yield	SWCNT or MWCNT
										C_2H_4							
Roberton	51	15 min	NH3	4/5×1.5 mbar	1/5×1.5 mbar		no	no	no	no	6 nm Ni+20 nm SiO_2	450 °C	plasma enhanced chemical vapor deposition	30 min			CNT or CNF
Hart	12			150 sccm	400 sccm	2.67	Ar	200 sccm	no	no	2 nm Fe + 30 nm Ta + 200 nm Cu+5 nm Ta	475 °C	three-zone atmospheric-pressure furnace, in a fused-silica tube with an internal diameter of 22 mm				
Hart	20			150 sccm	400 sccm	2.67	Ar	200 sccm	no	no	2 nm Fe + 30 nm Ta + 200 nm Cu+5 nm Ta	475 °C	three-zone hot wall tube furnace, the gases were heated in the first two zones and the growth happening at the third zone	30 min			
Hart	20		310 sccm H_2 + 300 sccm He	120 sccm	310 sccm	2.58	He	180 sccm	no	no	1 nm Fe + 10 nm Al_2O_3	525 °C	cold wall reactor				MWCNT
Zhang & Wei	23										Fe/Mo/vermiculite	550 °C	fluidized bed	30 min			
Roberton	2	5 min	200 sccm Ar/500 sccm H_2	500 sccm	200 sccm	0.40	Ar	500 sccm	no	no	2 nm Fe/ 10 nmAl_2O_3	600 °C	hot wall				
Roberton	2	5 min	200 sccm Ar/500 sccm H_2	500 sccm	200 sccm	0.40	Ar	500 sccm	no	no	1.7 nm Fe+0.3 nm Co/10 nm Al_2O_3	600 °C	hot wall				
Zhang & Wei	28	ramping to growth temperature	570 sccm Ar + 30 sccm H_2	100 sccm	30 sccm	0.30	Ar	570 sccm	no	no	ferrocene	600 °C	horizontal quartz tube, 35 mm in diameter and 1200 mm in length, two-stage furnace, CNT was grown at the second stage with 600 mm heat zone				
Roberton	2	5 min	200 sccm Ar/500 sccm H_2	500 sccm	200 sccm	0.40	Ar	500 sccm	no	no	2 nm Fe/ 10 nm Al_2O_3	650 °C	hot wall				
Roberton	2	5 min	200 sccm Ar/500 sccm H_2	500 sccm	200 sccm	0.40	Ar	500 sccm	no	no	1.7 nm Fe+0.3 nm Co/10 nm Al_2O_3	650 °C	hot wall				
Zhang & Wei	21										Fe/Mo/vermiculites	650 °C	comparison of fixed bed and fluidized bed, reactor has an inner diameter of 25 mm and a height of 700 mm;	60 min	7.5 cm		
Zhang & Wei	21	10 min	500 mL/min Ar + 50 mL/min H_2	100 mL/min	50 mL/min	0.50	Ar	500 mL/min	no	no	Fe/Mo/vermiculites	650 °C	fixed bed	60 min			
Zhang & Wei	21	10 min	500 mL/min Ar + 50 mL/min H_2	100 mL/min	50 mL/min	0.50	no known	upflow of the gas at a sufficient velocity to cause mobility	no	no	Fe/Mo/vermiculites	650 °C	fluidized bed	30 min			MWCNT
Zhang & Wei	23		H_2				Ar				Fe/Mo/vermiculite	650 °C	fluidized bed	30 min	10 um		
Zhang & Wei	23	0 min to 30 min	H_2								Fe/Mo/vermiculite	650 °C	fluidized bed	30 min			MWCNT
Zhang & Wei	23			space velocity : 0.05/min; 0.15/min; 0.30/min; 0.45/min; 0.60/min							Fe/Mo/vermiculite	650 °C	fluidized bed	5 min	0.5 to 1.5 um after 1-5 min synthesis	0.22 g CNT/gcat after 5 min	

Group	Paper #	annea l time	anneal gas	C_xH_y flow	H_2 flow	H_2/ C_xH_y	carrier gas	carrier gas flow	growth enhancer (Y/N)	Growth enhancer	catalyst	Tem.	reactor	growth time	terminal length	yield	SWCNT or MWCNT
Zhang & Wei	24	ramping to 650 °C	500 mL/min Ar + 20 mL/min H_2	100 mL/min	20 mL/min	0.20	Ar	500 mL/min	no	no	Fe/Mo/vermiculite	650 °C	fluidized bed inner diameter of 20 mm and a height of 300 mm				
Hart	11	2 min	310 sccm H_2 + 300 sccm He	120 sccm	310 sccm	2.58	He	180 sccm	no	no	1 nm Fe + 10 nm Al_2O_3	675 °C	cold wall reactor	15 min			MWCNT
Roberton	2	5 min	200 sccm Ar/500 sccm H_2	500 sccm	200 sccm	0.40	Ar	500 sccm	no	no	2 nm Fe/ 10 nm Al_2O_3	700 °C	hot wall				
Roberton	2	5 min	200 sccm Ar/500 sccm H_2	500 sccm	200 sccm	0.40	Ar	500 sccm	no	no	1.7 nm Fe+0.3 nm Co/10 nm Al_2O_3	700 °C	hot wall				
Zhang & Wei	28	ramping to growth temperature	570 sccm Ar + 30 sccm H_2	100 sccm	30 sccm	0.30	Ar	570 sccm	no	no	ferrocene	700 °C	horizontal quartz tube, 35 mm in diameter and 1200 mm in length, two-stage furnace, CNT was grown at the second stage with 600 mm heat zone				
Hart	11	2 min	310 sccm H_2 + 300 sccm He	120 sccm	310 sccm	2.58	He	180 sccm	no	no	1 nm Fe + 10 nm Al_2O_3	725 °C	cold wall reactor	15 min			
Hart	17	4 min	174 sccm He + 310 sccm H_2	120 sccm	310 sccm	2.58	He	174 sccm	yes	Alkynes at9.8×10^{-3} atm except vinyl acetylene (3×10^{-3} atm)	1 nm Fe + 10 nm Al_2O_3 + 300 nm SiO_2	725 °C	cold wall reactor	0.5 to 15 min			
Hata	27			1-12%			He		yes	water (20-900 ppm)	1.8 nm Fe+40 nm Al_2O_3	725 °C for plotting 725 °C to 825 °C	1 inch fully automated CVD system equiped with a telecentric optical system for in situ height measurements.				
Hata	27			1-12%			He		yes	water (20-900 ppm)	1.8 nm Fe+40 nm Al_2O_3	775 °C for plotting 725 °C to 825 °C	1 inch fully automated CVD system equiped with a telecentric optical system for in situ height measurements.				
Hata	25	750 °C	1:9 He/H_2	25 sccm C_2H_4			He	total flow 500 sccm	yes	water (50 to 500 ppm)	1.5 nm Fe + 40 nm Al_2O_3	725 °C for plotting 725 to 900 °C	1 inch fully automated CVD system				SWCNT
Hata	25	750 °C	1:9 He/H_2	25 sccm C_2H_4			He	total flow 500 sccm	yes	water (50 to 500 ppm)	1.5 nm Fe + 40 nm Al_2O_3	775 °C for plotting 725 to 900 °C	1 inch fully automated CVD system				
Hata	25	750 °C	1:9 He/H_2	25 sccm C_2H_4			He	total flow 500 sccm	yes	water (50 to 500 ppm)	1.5 nm Fe + 40 nm Al_2O_3	875 °C for plotting 725 to 900 °C	1 inch fully automated CVD system				
Zhang & Wei	26	ramping to 750 °C	250 sccm Ar+200 sccm H_2	100 sccm	200 sccm	2.00	Ar	250 sccm	yes	CO_2 0 mol%, 12.5 mol%, 22.5%, 30.4 mol%, 36.8 mol%	1 nm MgO+1 nm Fe + 10 nm Al_2O_3	730 °C	quartz tube with inner diameter of 30 mm and length of 1200 mm				
Roberton	2	5 min	200 sccm Ar/500 sccm H_2	500 sccm	200 sccm	0.40	Ar	500 sccm	no	no	2 nm Fe/ 10 nm Al_2O_3	750 °C	hot wall	15 min	480 +/- 35 um		MWCNT

Group	Paper #	annea l time	anneal gas	C_xH_y flow	H_2 flow	H_2/ C_xH_y	carrier gas	carrier gas flow	growth enhancer (Y/N)	Growth enhancer	catalyst	Tem.	reactor	growth time	terminal length	yield	SWCNT or MWCNT
Roberton	2	5 min	200 sccm Ar/500 sccm H_2	500 sccm	200 sccm	0.40	Ar	500 sccm	no	no	1.7 nm Fe+0.3 nm Co/10 nm Al_2O_3	750 °C	hot wall	15 min	817 +/- 56 um		MWCNT
Zhang & Wei	11	ramping to 750 °C	115 mL/min Ar	20 mL/min , 3mL/h CH_3CN was fed into the reactor by syringe pump	25 mL/min	1.25	Ar	115 mL/min	no	no	FeMgAl layered double hydroxides	750 °C	horizontal quartz tube (inner diameter of 25 mm)	10 min			Graphene/SW CNT
Zhang & Wei	17	10 min	250 sccm Ar+200 sccm H_2	100 sccm	200 sccm	2.00	Ar	250 sccm	no	no	1.0 nm MgO + 1.0 nm Fe + 10 nm Al_2O_3 +SiO_2	750 °C	horizontal quartz tube furnance	30 min	500 um using PP at 40 min growth time		MWCNT
Zhang & Wei	20	ramping to 750 °C + 10 min	ramping up under 300 mL/min + 10 min 100 mL/min Ar	300 mL/min	50 mL/min	0.17	Ar	100 mL/min	no	no	Fe/Mg/Al LDH	750 °C	horizontal quartz tube (inner diameter of 25 mm)				
Zhang & Wei	23										Fe/Mo/vermiculite	750 °C	fluidized bed	30 min			
Zhang & Wei	26	ramping to 750 °C	250 sccm Ar+200 sccm H_2	100 sccm	200 sccm	2.00	Ar	250 sccm	yes	CO_2 0 mol%, 6.5 mol%, 30.4 mol%	1 nm MgO+1 nm Fe + 10 nm Al_2O_3	750 °C	quartz tube with inner diameter of 30 mm and length of 1200 mm	60 min			
Hata	1			10-150 sccm	400 sccm	4.00	Ar or He	600 sccm	yes	water from 20 ppm to 500 ppm	Fe nanoparticles from $FeCl_3$ and sputtered metal thin film (Fe, Al/Fe, Al_2O_3 /Fe, Al_2O_3 /Co) on Si wafers, quartz, and metal foil	750 °C	hot wall CVD 1 inch diameter, 15 inch long heating zone	2 min			SWCNT
Hata	3			100 sccm	400 sccm	4.00	He	600 sccm	yes	150 ppm water	1.2 nm Fe + 10 nm Al_2O_3	750 °C	1 in. diameter quartz tube furnace	10-30 min	up to 2.2 mm		DWCNT
Hata	4			10-150 sccm			He	He+ H_2 =1000 sccm	yes	water (20-500 ppm)	Fe+30 nm Al_2O_3 +600 nm SiO_2	750 °C	hot wall CVD				
Hata	6			100 sccm	no	0.00	He	1000 sccm	yes	water(100-150 ppm)	Fe nanoparticles made by colloidal synthesis (average size 3.2 nm) dispersed in n-hexane and deposited onto Al_2O_3 by spin coating	750 °C	1 inch tube furnace				
Hata	9		He/H_2	50 sccm					yes	water (100 ppm)	1.5 nm Fe + 50 nm SiO_2 on 50 nm diameter on Cu TEM grid	750 °C		1 min			
Hata	9		He/H_2	10 sccm					yes	water (100 ppm)	1.5 nm Fe + 50 nm SiO_2 on 50 nm diameter SiO_2 on Cu TEM grid	750 °C			up to 5 mm		
Hata	10			75 sccm			He+H_2	total 1000 sccm	yes	water (100-150 ppm)	1 nm Fe+10 nm Al_2O_3	750 °C					
Hata	10			20 sccm			He+H_2	total 1000 sccm	yes	water (100-150 ppm)	1 nm Fe+10 nm Al_2O_3	750 °C					
Hata	12			100 sccm	no	0.00	He with small water vapor	900 sccm	yes	water (~0 to ~500 ppm)	1 nm Fe+10 nm Al_2O_3	750 °C	1 inch quartz lateral tube furnace but with different gas flow directions: conventional lateral-flow growth, water top-flow growth, and top-flow growth				SWCNT
Hata	12			10 sccm	no	0.00	He with small water vapor	90 sccm	yes	water (~0 to ~500 ppm)	1 nm Fe+10 nm Al_2O_3	750 °C	gas shower system for top-flow growth	10 min	500-1000 um		SWCNT, DWCNT and MWCNT
Hata	19		H_2 /He (40%/60%)	10%					yes	water (100-150 ppm)	Fe/AlO_x	750 °C	hot wall reactor	1 min			

Group	Paper #	annea l time	anneal gas	C_xH_y flow	H_2 flow	H_2/ C_xH_y	carrier gas	carrier gas flow	growth enhancer (Y/N)	Growth enhancer	catalyst	Tem.	reactor	growth time	terminal length	yield	SWCNT or MWCNT
Hata	19	5 min	H_2 /He				He				1.5 nm/10 nm AlO_x on 50 nm SiO_2 nanoballs on TEM grid for "Ball CVD"	750 °C		10 min			
Hata	21	550-750 °C	90% H_2 in He	1%			He	99%			Fe film (0.5-2.5 nm) and Al film (0.5-2.0 nm) on oxygen plasma treated 5 nm Aluminum	750 °C	hot wall reactor				SWCNT, DWCNT and TWCNT
Hart	2				H_2 /C2H4 ratio not mention						Mo/Fe/Al_2O_3	750 °C	single-zone atmospheric pressure quartz tube furnace with inside diameter of 22 mm and a 30 scm long heating zone				
Hart	2				H_2 /C2H4 ratio not mention						Fe/Al_2O_3	750 °C	single-zone atmospheric pressure quartz tube furnace with inside diameter of 22 mm and a 30 scm long heating zone	15 min	0.9 mm		MWCNT
Hart	3	1-5 min	Ar+H_2	100 sccm	500 sccm	5.00	Ar	200 sccm	no	no	1.2 nm Fe + 20 nm Al_2O_3	750 °C	single-zone atmospheric pressure quartz tube furnace with inside diameter of 22 mm and a 30 scm long heating zone	60 min	1.8 mm		MWCNT
Hart	3	1-5 min	Ar+H_2	100 sccm	500 sccm	5.00	Ar	200 sccm	no	no	1.2 nm Fe + 20 nm Al_2O_3	750 °C	single-zone atmospheric pressure quartz tube furnace with inside diameter of 22 mm and a 30 scm long heating zone	15 min			
Hart	3	1-5 min	Ar+H_2	10-75 sccm	500 sccm	10.00	Ar	200 sccm	no	no	1.2 nm Fe + 20 nm Al_2O_3	750 °C	single-zone atmospheric pressure quartz tube furnace with inside diameter of 22 mm and a 30 scm long heating zone	15 min			
Hart	3	1-5 min	Ar+H_2	75-200 sccm	500 sccm	3.33	Ar	200 sccm	no	no	1.2 nm Fe + 20 nm Al_2O_3	750 °C	single-zone atmospheric pressure quartz tube furnace with inside diameter of 22 mm and a 30 scm long heating zone				
Hart	6										1.2 nm Fe + 10 nm Al_2O_3	750 °C	hot wall CVD				MWCNT
Hart	6										iron oxide nan°C luster arryas templated by a PS-b-PAA micellear film onto an Al_2O_3 -coated Si substrate	750 °C	hot wall CVD				
Hart	14	0-10 min	400 sccm He + 1600 sccm H_2	400 sccm	1600 sccm	4.00	He	400 sccm	no	no	ZrO_2	750 °C	three-zone Lindberg/Blue M furnace with a 62-cm heated length using 50-mm inner diameter fused quartz pr°C ess tubes with a length of 138 cm	10 min+ 20 min			
Hart	16		He/H_2						no	no	1 nm Fe + 10 nm Al_2O_3	750 °C	cold wall reactor				MWCNT
Hart	24	5 min	400 sccm H_2 + 150 sccm Ar	100 sccm	400 sccm	4.00	Ar	150 sccm	no	no	1.2 nm Fe + 10 nm A_2O_3	750 °C	2 in. quartz tube furnace at atmosphere				
Ajayan	27			100 sccm	400 sccm	4.00	Ar	500 sccm	yes	water (carried by 10 sccm H_2)	1.5 nm Fe + 10 nm Al_2O_3	750 °C	hot wall CVD				
Hata	2		Ar and H_2 (total 1000 sccm)	10 sccm					no	no	Fe and Co-Mo catalyst	750 °C	hot wall CVD 1 inch diameter, 15 inch long heating zone	15 min			SWCNT

Group	Paper #	annea l time	anneal gas	C_xH_y flow	H_2 flow	H_2/ C_xH_y	carrier gas	carrier gas flow	growth enhancer (Y/N)	Growth enhancer	catalyst	Tem.	reactor	growth time	terminal length	yield	SWCNT or MWCNT
Zhang & Wei	2	ramping to 750 °C	150 mL/min Ar + 120 mL/min H_2	60 mL/min C2H4 + 50 mL/min NH3 for 30 min at 750 °C , after ramping to 950 °C , 120 mL/min CH4+150 mL/min Ar for 30 min			Ar	150 mL/min ramp from 750 °C to 950 °C	no	no	Fe/Mo bifunctional catalyst	750 °C for CNT growth, 950 °C for graphene growth	hot wall horizontal quartz tube	15 min			N-doped SWCNT/Graphene Hybrids
Ajayan	16				15% of Ar/H_2 mixture		Ar	85% of Ar/H_2 mixture	Yes	water with a dew point of -20 °C	1-3 nm Fe + 5-20 nm Al	750 °C for plotting 750-800 °C	hot wall CVD				
Zhang & Wei	26	ramping to 750 °C	250 sccm Ar+200 sccm H_2	100 sccm	200 sccm	2.00	Ar	250 sccm	Yes	CO2 0 mol%, 12.5 mol%, 22.5%, 30.4 mol%, 36.8 mol%	1 nm MgO+1 nm Fe + 10 nm Al_2O_3	770 °C	quartz tube with inner diameter of 30 mm and length of 1200 mm				
Hart	8			150 sccm	no	0.00	Ar	600 sccm	no	no	1.2 nm Fe + 10 nm Al_2O_3	770 °C	three-zone atmospheric-pressure furnace, in a fused-silica tube with an internal diameter of 22 mm	15 min			MWCNT
Hart	8			150 sccm	400 sccm	2.67	Ar	200 sccm	no	no	1.2 nm Fe + 10 nm Al_2O_3	770 °C	three-zone atmospheric-pressure furnace, in a fused-silica tube with an internal diameter of 22 mm	2.5 to 30 min			
Hart	9	10 min	400 H_2 + 100 sccm He	100 sccm	400 sccm	4.00	He	100 sccm	no	no	1 nm Fe + 10 nm Al_2O_3	775 °C	horizontal quartz tube furnace (22 mm inner diameter, 12 in. heated length)				
Hart	11	2 min	310 sccm H_2 + 300 sccm He	120 sccm	310 sccm	2.58	He	180 sccm	no	no	1 nm Fe + 10 nm Al_2O_3	775 °C	cold wall reactor	15 min			
Hart	15	10 min	100 sccm He + 400 sccm H_2	100 sccm	400 sccm	4.00	He	100 sccm	no	no	1 nm Fe + 10 nm Al_2O_3	775 °C	single-zone atmospheric pressure tube furnace				MWCNT
Hart	18			100 sccm	400 sccm	4.00	He	100 sccm	no	no	1 nm Fe + 10 nm Al_2O_3	775 °C	horizontal tube furnace (22 mm inner diameter, 300 mm heated length)				
Hart	22	2 min	310 sccm H_2 + 300 sccm He	120 sccm	310 sccm	2.58	He	180 sccm	no	no	1 nm Fe + 10 nm Al_2O_3 + 300 nm SiO_2	775 °C	cold wall reactor				
Hart	26	10 min	400 sccm He + 100 sccm H_2	100 sccm	100 sccm	1.00	He	100 sccm	no	no	1 nm Fe + 10 nm Al_2O_3 +300 nm SiO_2	775 °C	hot wall CVD, 300 mm heated region	10 min			
Hart	27	10 min	400 sccm He + 100 sccm H_2	100 sccm	100 sccm	1.00	He	100 sccm	no	no	1 nm Fe + 10 nm Al_2O_3 +300 nm SiO_2	775 °C	hot wall CVD, 300 mm heated region	10 min			
Hart	27	10 min	400 sccm He + 100 sccm H_2	100 sccm	100 sccm	1.00	He	100 sccm	yes	O_2 and generate H_2O	1 nm Fe + 10 nm Al_2O_3 +300 nm SiO_2	775 °C	hot wall CVD, 300 mm heated region	20 min			
Hart	28	10 min	400 H_2 + 100 sccm He	100 sccm	100 sccm	1.00	He	400 sccm	no	no	Blade casting ferrofluid solution on 10 nm Al_2O_3 + 300 nm SiO_2	775 °C	Horizontal tube furnace (22 mm ID, 300 mm heated length) at atmospheric pressure	15 min			

Group	Paper #	annea l time	anneal gas	C_xH_y flow	H_2 flow	H_2/ C_xH_y	carrier gas	carrier gas flow	growth enhancer (Y/N)	Growth enhancer	catalyst	Tem.	reactor	growth time	terminal length	yield	SWCNT or MWCNT
Hart	29	10 min	100 sccm He + 400 sccm H_2	100 sccm	100 sccm	1.00	He	400 sccm	no	no	catalyst + 10 nm Al_2O_3 + 300 nm SiO_2	775 °C	horizontal tube furnace with a 25 mm OD quartz tube (22 mm ID, 300 mm heated length) at atmospheric pressure				
Hart	30	10 min	400 sccm H_2 + 100 sccm He	100 sccm	100 sccm	1.00	He	400 sccm	no	no	1 nm Fe + 10 nm Al_2O_3 + 300 nm SiO_2	775 °C	hot wall tube furnace with rapid sample insertion mechanism				
Ajayan	28				15% of Ar/H_2 mixture		Ar	85% of Ar/H_2 mixture	yes	water	1.5 nm Fe + 10 nm Al	775 °C	hot wall CVD				
Hata	29	15 min+5 min	5%×2000 sccm H_2 + 95%×2000 sccm He after 15 min, then various water (0-50 ppm) and various hydrogen (0-2%) was introduced to the reactor for 5 min	0.025%-0.25%	no		He		no	no	Fe nanoparticle on SiO_2	780 °C	quartz tube furnace (inner diameter 80 mm)	15 min			MWCNT
Zhang & Wei	26	ramping to 750 °C	250 sccm Ar+200 sccm H_2	100 sccm	200 sccm	2.00	Ar	250 sccm	yes	CO_2 0 mol%, 12.5 mol%, 22.5%, 30.4 mol%, 36.8 mol%	1 nm MgO+1 nm Fe + 10 nm Al_2O_3	790 °C	quartz tube with inner diameter of 30 mm and length of 1200 mm				
Zhang & Wei	34	ramping to 800 °C	760 sccm Ar + 40 sccm H_2	100 sccm	40 sccm	0.40	Ar	760 sccm	no	no	ferrºC ene, substrates consisting of 50% SiO_2 , 30% Al_2O_3 , and 20% ZrO2	800 °C	horzontal quartz tube, 25 mm in diameter and 1200 mm in length with two-stage furnace	15 min			CNT species depends on the Fe load
Hata	28			0-3.0 $\times 10^{-3}$, peak at 6.0×10^{-4} mol/cm 2/min					yes	water	1.8 nm Fe+40 nm Al_2O_3	800 °C	hot wall CVD	2 min			SWCNT
Hart	23			120 sccm'	310 sccm	2.58	He	180 sccm	no	no	1 nm Fe + 10 nm Al_2O_3 +300 nm SiO_2	800 °C	cold wall reactor	15 min			
Hart	25			120 sccm'	310 sccm	2.58	He	180 sccm	no	no	1 nm Fe + 10 nm Al_2O_3 +300 nm SiO_2	800 °C	cold wall reactor	10 min			
Zhang & Wei	28	ramping to growth temperature	570 sccm Ar + 30 sccm H_2	100 sccm	30 sccm	0.30	Ar	570 sccm	no	no	Ferrocene	800 °C	horizontal quartz tube, 35 mm in diameter and 1200 mm in length, two-stage furnace, CNT was grown at the second stage with 600 mm heat zone				

Group	Paper #	annea l time	anneal gas	C_xH_y flow	H_2 flow	H_2/ C_xH_y	carrier gas	carrier gas flow	growth enhancer (Y/N)	Growth enhancer	catalyst	Tem.	reactor	growth time	terminal length	yield	SWCNT or MWCNT
Hata	16	15 min	200 sccm He + 1800 sccm H_2	100 sccm	900 sccm	9.00	He	1000 sccm	yes	water (100 ppm), water vapor of 100 ppm was supplied by passing 1000 sccm He carrier gas through a water bubbler	0.8-3.0 nm Fe + 40 nm Al_2O_3 + 600 nm SiO_2	810 °C	3 in. quartz tube furnace				
Hart	4	5 min	400 sccm H_2 + 140 sccm Ar	115 sccm	400 sccm	3.48	Ar or CO	100 sccm	no	no	1 nm Fe + 10 nm Al_2O_3	810 °C	cold wall reactor, suspended silicon platform heater, 300 mm length, 48 mm internal diameter, 52 mm outer diameter	15 min			tangled films of SWCNT
Hart	5	5 min	400 sccm H_2 + 140 sccm Ar	115 sccm	400 sccm	3.48	Ar	140 sccm	no	no	1 nm Fe + 10 nm Al_2O_3	825 °C	cold wall reactor, suspended silicon platform heater, 300 mm length, 48 mm internal diameter, 52 mm outer diameter				MWCNT
Hart	7		310 sccm H_2 + 300 sccm He	120 sccm	310 sccm	2.58	He	180 sccm	no	no	1 nm Fe + 10 nm Al_2O_3 +100 nm SiO_2	825 °C	cold wall reactor	15 min			MWCNT
Hart	9	2 min	310 sccm H_2 + 300 sccm He	120 sccm	310 sccm	2.58	He	180 sccm	no	no	1 nm Fe + 10 nm Al_2O_3	825 °C	cold wall reactor	30 min	0.9 mm in the moving-growth system		MWCNT
Hart	10			200 sccm	600 sccm	3.00	He	500 sccm	no	no	1 nm Fe + 10 nm Al_2O_3	825 °C	cold wall reactor				MWCNT
Hart	11	2 min	310 sccm H_2 + 300 sccm He	120 sccm	310 sccm	2.58	He	180 sccm	no	no	1 nm Fe + 10 nm Al_2O_3	825 °C	cold wall reactor	15 min			
Hart	19	10 min	400 sccm H_2 + 100 sccm He	100 sccm	400 sccm	4.00	He	100 sccm	yes	ethanol (C_2H_5OH), 50 sccm He was diverted through the bubbler	Fe_2O_3 nanoparticles on Montmorillonite (MTM) and Poly (dyallyldimethyl ammonium chloride) (PDDA)	825 °C	single-zone atmospheric pressure quartz tube furnace with inside diameter of 22 mm and a 30 scm long heating zone	15 min			
Hata	26	500-950 °C	90% H_2 in He at 500-4000 sccm	50 sccm	no	0.00	He	950 sccm	yes	~100 ppm water	1.5 nm Fe + 30 nm AlOx	840 °C	hot wall CVD				
Zhang & Wei	23										Fe/Mo/vermiculite	850 °C	fluidized bed	30 min			
Hart	11	2 min	310 sccm H_2 + 300 sccm He	120 sccm	310 sccm	2.58	He	180 sccm	no	no	1 nm Fe + 10 nm Al_2O_3	875 °C	cold wall reactor	15 min			
Zhang & Wei	23										Fe/Mo/vermiculite	950 °C	fluidized bed	30 min			
Hart	1	1 min	500 sccm H_2 + 200 sccm Ar	100 sccm	500 sccm	5.00	Ar	200 sccm	no	no	1.2 nm Fe + 10 nm Al_2O_3	not mention ed	single zone atmospheric pressure quartz tube furnace				

Group	Paper #	annea l time	anneal gas	C_xH_y flow	H_2 flow	H_2/ C_xH_y	carrier gas	carrier gas flow	growth enhancer (Y/N)	Growth enhancer	catalyst	Tem.	reactor	growth time	terminal length	yield	SWCNT or MWCNT
Hata	22	15 min	200 sccm He + 1800 sccm H_2	100 sccm	900 sccm	9.00	He	1000 sccm	yes	water (100 ppm), water vapor of 100 ppm was supplied by passing 1000 sccm He carrier gas through a water bubbler water (50 to 500 ppm)	0.8-3.0 nm Fe + 40 nm Al_2O_3 + 600 nm SiO_2		3 inch quartz tube furnace	1 min			
Hata	24			25 sccm			He	total flow 500 sccm	yes		1.5 nm Fe + 40 nm Al_2O_3						
Hart	13	2min	70 sccm He+330 sccm	70 sccm	330 sccm	4.71	no	no	no	no	1.2 nm Fe + 10 nm Al_2O_3 +600 um		cold wall reactor	15 min			
Zhang & Wei	3	ramping to 950 °C	500 mL/min Ar	300 mL/min for C2H4 and 100 mL/min NH_3	50 mL/min	0.17	Ar	200 mL/min	no	no	FeMoMgAl layered double hydroxides (LDHs)			15 min		0.59 gG/SWCNTs/gcat to 0.97 gG/SWCNTs/gcat	Graphene/SWCNT
										C_2H_2							
Roberton	51		NH_3	4/5×1.5 mbar	1/5×1.5 mbar		no	no	no	no	6 nm Ni+20 nm SiO_2	120 °C	plasma enhanced chemical vapor deposition	1 h			CNT or CNF
Roberton	52		NH_3	30 sccm C_2H_2	200 sccm NH_3		no	no	no	no	6 nm Ni + 70 nm Cr	200 °C	plasma enhanced chemical vapor deposition				
Roberton	51		NH_3	4/5×1.5 mbar	1/5×1.5 mbar		no	no	no	no	6 nm Ni+20 nm SiO_2	270 °C	plasma enhanced chemical vapor deposition				CNT or CNF
Roberton	49	15 min	NH_3 at 0.6 mbar to 20 mbar or H_2 at 0.6 mbar to 100 mbar		no	0.00	no	no	no	no	Fe or Al/Fe+ Al+SiO_2	350 °C	thermal CVD at cold wall conditions				
Roberton	49	15 min	NH_3 at 0.6 mbar to 20 mbar or H_2 at 0.6 mbar to 100 mbar		no	0.00	no	no	no	no	0.3 nm Fe+ Al+SiO_2	400 °C	thermal CVD at cold wall conditions				
Roberton	49	15 min	NH_3 at 0.6 mbar to 20 mbar or H_2 at 0.6 mbar to 100 mbar	5 sccm	no	0.00	no	no	no	no	0.1 nm Fe + Al+SiO_2	420 °C	thermal CVD at cold wall conditions	5 min			
Roberton	3	ramping to 450 °C	200 sccm NH_3	200 sccm C_2H_2	no	0.00	no	no	no	no	2.5 nmCo+0.25, 0.50 or 1.0 nm Al+5.0 nm Mo+40 nm Cu on 200 nm SiO_2	450 °C	cold wall	3min	300 nm		MWCNT
Roberton	8	ramping up to 450 °C with 3 °C /s	H_2 or NH3				Ar		no	no	Co (1.5 nm, 2.5 nm, 4.0 nm) + Mo (0 or 0.8 nm)+Ti (0, 3.0 nm or 5.0 nm)+ Cu (40 nm)	450 °C	cold wall				MWCNT
Roberton	8		200 sccm NH_3	200 sccm C_2H_2	no	0.00	no	no	no	no	2.5 nm Co+3.0 nm Ti	450 °C	cold wall	3 min	0.45 um		MWCNT
Roberton	8		200 sccm NH_3	200 sccm C_2H_2	no	0.00	no	no	no	no	2.5 nm Co+5 nm Ti	450 °C	cold wall	3 min	0.78 um		MWCNT

Group	Paper #	annea l time	anneal gas	C_xH_y flow	H_2 flow	H_2/ C_xH_y	carrier gas	carrier gas flow	growth enhancer (Y/N)	Growth enhancer	catalyst	Tem.	reactor	growth time	terminal length	yield	SWCNT or MWCNT
Roberton	8		200 sccm NH_3	200 sccm C_2H_2	no	0.00	no	no	no	no	2.5 nm Co+0.8 nm Mo+3.0 nm Ti	450 °C	cold wall	3 min	0.21 um		MWCNT
Roberton	8		200 sccm NH_3	200 sccm C_2H_2	no	0.00	no	no	no	no	2.5 nm Co+0.8 nm Mo+5.0 nm Ti	450 °C	cold wall	3 min	0.40 um		MWCNT
Roberton	8		200 sccm NH_3	200 sccm C_2H_2	no	0.00	no	no	no	no	2.5 nm Co+5.0 nm Ti	450 °C	cold wall	3 min	0.92 um		MWCNT
Roberton	8		200 sccm NH_3	200 sccm C_2H_2	no	0.00	no	no	no	no	2.5 nm Co+5.0 nm Ti	450 °C	cold wall	10 min	1.3 um		MWCNT
Roberton	8		200 sccm NH_3	200 sccm C_2H_2	no	0.00	no	no	no	no	2.5 nm Co+5.0 nm Ti	450 °C	cold wall	30 min	1.5 um		MWCNT
Roberton	8		200 sccm NH_3	200 sccm C_2H_2	no	0.00	no	no	no	no	2.5 nm Co+0.8 Mo+5.0 nm Ti	450 °C	cold wall	3 min	0.4 um		MWCNT
Roberton	8		200 sccm NH_3	200 sccm C_2H_2	no	0.00	no	no	no	no	2.5 nm Co+0.8 Mo+5.0 nm Ti	450 °C	cold wall	10 min	0.5 um		MWCNT
Roberton	8		200 sccm NH_3	200 sccm C_2H_2	no	0.00	no	no	no	no	2.5 nm Co+0.8 Mo+5.0 nm Ti	450 °C	cold wall	30 min	0.89 um		MWCNT
Roberton	8		200 sccm NH_3	200 sccm C_2H_2	no	0.00	no	no	no	no	2.5 nm Co+0.8 Mo+5.0 nm Ti	450 °C	cold wall	100 min	1.8 um		MWCNT
Roberton	10	5 min	1000 sccm Ar + 500 sccm H_2	10 sccm C_2H_2	500 sccm	50.00	Ar	1000 sccm Ar	no	no	1 nm Fe/10 nm Al_2O_3	450 °C	hot wall reactor	10 min	0		
Roberton	10	5 min	1000 sccm Ar + 500 sccm H_2	10 sccm C_2H_2	500 sccm	50.00	Ar	1000 sccm Ar	no	no	1 nm Fe/10 nm plasma treated Al_2O_3	450 °C	hot wall reactor	10 min	0		
Roberton	14	ramping up to 400 to 550 °C	200 sccm NH_3	200 sccm C_2H_2	no	0.00	no	no	no	no	2.5 nm Co+0.8 nm Mo+5 nm Ti	450 °C	cold wall reactor	3 min	0.38 um		MWCNT
Roberton	14	ramping up to 400 to 550 °C	200 sccm NH_3	200 sccm C_2H_2	no	0.00	no	no	no	no	2.5 nm Co+0.3 nm Mo+5 nm Ti	450 °C	cold wall reactor	3 min	0.58 um		MWCNT
Roberton	14	ramping up to 400 to 550 °C	200 sccm NH_3	200 sccm C_2H_2	no	0.00	no	no	no	no	2.5 nm Co+5nm Ti	450 °C	cold wall reactor	3 min	0.83 um		MWCNT
Roberton	51	15 min	NH3	4/5×1.5 mbar	1/5×1.5 mbar		no	no	no	no	6 nm Ni+20 nm SiO_2	450 °C	plasma enhanced chemical vapor deposition	30 min			CNT or CNF
Roberton	19	480 °C	1 mbar NH_3	20 mbar C_2H_2	no	0.00	no	no	no	no	1 nm Fe, Ni, Co on momo-Si	480 °C	cold wall reactor				
Roberton	19	480 °C	1 mbar NH_3	20 mbar C_2H_2	no	0.00	no	no	no	no	1 nm Fe, Ni, Co on poly-Si	480 °C	cold wall reactor				
Roberton	27	5 min	100 mbar H_2 and 50 W dc plasma	0.5 mbar C_2H_2	no	0.00	no	no	no	no	0.5 nm or 1 nm Ni, Co, Fe+100 nm TiN + 200 nm SiO_2	480 °C	cold wall	15 min			
Roberton	14	ramping up to 400 to 550 °C	200 sccm NH_3	200 sccm C_2H_2	no	0.00	no	no	no	no	2.5 nm Co+0.8 nm Mo+5 nm Ti	500 °C	cold wall reactor				
Roberton	32		0.5-0.8mbar NH_3	$1\text{-}5\times10^{-3}$ mbar C_2H_2	no	0.00	no	no	no	no	Ni, Au, Fe, or Pd+ 30 nm SiOx onto TEM grids	500 °C	cold wall chamber	5 min	200 um-1400 um		MWCNT
Roberton	39	5 min	NH_3	2.5×10^{-3} mbar	no	0.00	no	no	no	no	0.5 nm Fe+10 nm Al_2O_3 or SiO_2	500 °C	cold wall reactor				
Roberton	49	15 min	NH_3 at 0.6 mbar to 20 mbar or H_2 at 0.6 mbar to 100 mbar	5 sccm	no	0.00	no	no	no	no	0.1 nm Fe + Al+SiO_2 or 0.3 nm Fe or Al/Fe (0.5 nm)/Al (top, 0.2 nm)	500 °C	thermal CVD at cold wall conditions				
Roberton	51		NH3	4/5×1.5 mbar	1/5×1.5 mbar		no	no	no	no	6 nm Ni+20 nm SiO_2	500 °C	plasma enhanced chemical vapor deposition				
Roberton	17	ramping up to 520 °C in 10 °C /s	192 sccm H_2	8 sccm C_2H_2	192 sccm	24.00	no	no	no	no	0.3 nm to 3 nm Fe/Al_2O_3	520 °C	cold wall reactor	3 min			DWCNT and MWCNT

Group	Paper #	annea l time	anneal gas	C_xH_y flow	H_2 flow	H_2/ C_xH_y	carrier gas	carrier gas flow	growth enhancer (Y/N)	Growth enhancer	catalyst	Tem.	reactor	growth time	terminal length	yield	SWCNT or MWCNT
Hart	14	15 min	0.1 mbar H_2	10^{-2} mbar in the first 10 min, then 1/6×0.2 mbar in the next 20 min	none in the first 10 min, then 5/6*0.2 mbar in the next 20 min	5.00	no	no	no	no	ZrO2	530 °C	low-pressure cold wall	20 min			
Roberton	14	ramping up to 400 to 550 °C	200 sccm NH_3	200 sccm C_2H_2	no	0.00	no	no	no	no	2.5 nm Co+0.8 nm Mo+5 nm Ti	550 °C	cold wall reactor				
Roberton	24	3 min	20 sccm Ar/50 sccm H_2	1 sccm C_2H_2	50 sccm	50.00	Ar	20 sccm Ar	no	no	1.1 nm Fe + 10~20 nm Al_2O_3	550 °C	hot wall reactor	20-30 min			
Roberton	26	3 min	500 sccm H_2 /200 sccm Ar	10 sccm C_2H_2	500 sccm	50.00	Ar	200 sccm	no	no	1.1 nm Fe + 100 nm Ta	550 °C	Atmospheric pressure hot wall reactor	40 min			
Roberton	50	15 min	0.5 mbar NH_3	50 sccm C_2H_2	200 sccm NH_3		no	no	no	no	Fe, Co, Ni catalyst film	550 °C	plasma enhanced chemical vapor deposition	10 min			
Homma	29			3 Pa/h	no	0.00	no	no	no	no	0.5 nm Co	550 °C	Environmental TEM				
Roberton	33			10 sccm C_2H_2	500 sccm	50.00	Ar	200 sccm Ar	no	no	0.5-1nm Fe+10 nm Al_2O_3 +200 nm thermal SiO_2	560 °C	2 inch hot wall reactor				
Roberton	26	3 min	500 sccm H_2 /200 sccm Ar	10 sccm C_2H_2	500 sccm	50.00	Ar	200 sccm	no	no	1.1 nm Fe + 100 nm Ta	565 °C	Atmospheric pressure hot wall reactor				
Roberton	26	3 min	500 sccm H_2 /200 sccm Ar	10 sccm C_2H_2	500 sccm	50.00	Ar	200 sccm	no	no	1.1 nm Fe + 100 nm Ta	575 °C	Atmospheric pressure hot wall reactor				
Roberton	26	no	no	$4×10^{-4}$ mbar C_2H_2	no	0.00	no	no	no	no	Fe+100 nm Ta	580 °C	Low pressure cold wall	10 min			
Roberton	26	5 min	H_2 plasma	0.8 mbar C_2H_2	no	0.00	no	no	no	no	1.1 nm Fe + 100 nm Ta	580 °C	cold wall	10 min			
Roberton	29	5 min	200 sccm H_2	5 sccm C_2H_2	195 sccm	39.00	no	no	no	no	1 nm Fe+ 25 nm $CoSi_2$	580 °C	cold wall reactor		<10 um		MWCNT
Roberton	39	5 min		$8×10^{-5}$ mbar	no	0.00	no	no	no	no	0.5 nm Fe+10 nm Al_2O_3	580 °C	high vacuum cold wall				
Roberton	39	5 min	NH3	$2.5×10^{-3}$ mbar	no	0.00	no	no	no	no	0.5 nm Fe+10 nm Al_2O_3 or SiO_2	580 °C	cold wall reactor				
Roberton	40		H_2 sputtering	8×10-4 mbar C_2H_2	no	0.00	no	no	no	no	0.5 nm Fe+150 nm SiO_2	580 °C	UHV cold wall	5 min			
Roberton	45	480 °C	1 mbar NH_3	$2×10^{-7}$ mbar C_2H_2	no	0.00	no	no	no	no	Ni or Fe on SiOx	580 °C	ETEM				
Roberton	5	10 min at 600, 650, 700 °C	10^{-3} mbar H_2	10^{-2} mbar	no	0.00	no	no	no	no	0.5 nm, 1 nm, 2 nm, 3 nm, 4 nm, 5 nm Fe on TiN and poly-crystalline PtSi films	600 °C	cold wall	15 min			MWCNT
Roberton	10	5 min	1000 sccm Ar + 500 sccm H_2	10 sccm C_2H_2	500 sccm	50.00	Ar	1000 sccm Ar	no	no	1 nm Fe/10 nm Al_2O_3	600 °C	hot wall reactor	10 min	620 um		
Roberton	10	5 min	1000 sccm Ar + 500 sccm H_2	10 sccm C_2H_2	500 sccm	50.00	Ar	1000 sccm Ar	no	no	1 nm Fe/10 nm plasma treated Al_2O_3	600 °C	hot wall reactor	10 min	720 um		
Roberton	19	600 °C	1 mbar NH_3	20 mbar C_2H_2	no	0.00	no	no	no	no	1 nm Fe, Ni, Co on Si	600 °C	cold wall reactor	15 min			DWCNT and MWCNT
Roberton	19	600 °C	1 mbar NH_3	20 mbar C_2H_2	no	0.00	no	no	no	no	1 nm Fe, Ni, Co on Si	600 °C	cold wall reactor				
Roberton	22	3 min at 600 °C	500 sccm H_2	20 sccm C_2H_2	480 sccm	24.00	no	no	no	no	20 nm CoSi2 + 200 nm polycrystalline silicon	600 °C	cold wall reactor	3 min	6.0-9.9 um		SWCNT
Roberton	26	3 min	500 sccm H_2 /200 sccm Ar	10 sccm C_2H_2	500 sccm	50.00	Ar	200 sccm	no	no	1.1 nm Fe + 100 nm Ta	600 °C	Atmospheric pressure hot wall reactor				
Roberton	27	5 min	100 mbar H_2 and 50 W dc plasma	0.5 mbar C_2H_2	no	0.00	no	no	no	no	0.5 nm or 1 nm Ni, Co, Fe+100 nm TiN + 200 nm SiO_2	600 °C	cold wall				

Group	Paper #	annea l time	anneal gas	C_xH_y flow	H_2 flow	H_2/ C_xH_y	carrier gas	carrier gas flow	growth enhancer (Y/N)	Growth enhancer	catalyst	Tem.	reactor	growth time	terminal length	yield	SWCNT or MWCNT
Roberton	40		H_2 sputtering	4×10^{-8} mbar C_2H_2	no	0.00	no	no	no	no	0.4 nm Fe+150 nm SiO_2	600 °C	UHV cold wall	5 min			
Roberton	44	5 min	100 sccm H_2 plasma	100 sccm C_2H_2	no	0.00	no	no	no	no	1 nm Ni on HGTS	600 °C		10 min			MWCNT
Roberton	47	Ni islands formed upon raising the temperature	no	8×10^{-3} mbar C_2H_2	no	0.00	no	no	no	no	Ni on SiO_2 nanopower on TEM grids	600 °C	ETEM	15 min			
Homma	20			1/2 of total flow	1/2 of total flow	1.00	no	no	no	no	1 nm Fe + SiO_2	600 °C	in situ TEM, low pressure				
Homma	24			1/2 of total flow	1/2 of total flow	1.00	no	no	no	no	Fe and Mo in SiO_2	600 °C	Environmental TEM	30 min			
Roberton	45			8×10^{-3} mbar C_2H_2	no	0.00	no	no	no	no	Ni on SiOx	615 °C	ETEM	15 min			SWCNT
Roberton	18	heat to 620 °C , 5-45 min	5×10^{-3} mbar NH_3	1×10^{-3} mbar C_2H_2	5×10^{-3} mbar NH_3		no	no	no	no	1 nm Fe + 2 nm Ta	620 °C	cold wall reactor	15-45 min			MWCNT
Roberton	24	3 min	20 sccm Ar/50 sccm H_2	1 sccm C_2H_2	50 sccm	50.00	Ar	20 sccm Ar	no	no	1.1 nm Fe + 10~20 nm Al_2O_3	625 °C	hot wall reactor				
Roberton	26	3 min	500 sccm H_2 /200 sccm Ar	10 sccm C_2H_2	500 sccm	50.00	Ar	200 sccm	no	no	1.1 nm Fe + 100 nm Ta	625 °C	Atmospheric pressure hot wall reactor				
Roberton	5	10 min at 600, 650, 700 °C	10^{-3} mbar H_2	10^{-2} mbar	no	0.00	no	no	no	no	0.5 nm, 1 nm, 2 nm, 3 nm, 4 nm, 5 nm Fe on TiN and poly-crystalline PtSi films	650 °C	cold wall	15 min			
Roberton	15	5 min	1000 sccm Ar + 500 sccm H_2	5, 8, 10, 15 sccm	500 sccm	50.00	Ar	1000 sccm Ar	no	no	0.5, 1.0, or 2.0 nm high purity Ni, Co, or Fe or a combination of two of them (in equal proportions) and same total thickness	650 °C	hot wall reactor	5, 10, 15 min			
Roberton	16	3 min	500 sccm H_2	20 sccm C_2H_2	480 sccm	24.00	no	no	no	no	1-4 nm Fe on 6 nm Al_2O_3	650 °C	cold wall reactor	5 min			MWCNT
Roberton	24	3 min	20 sccm Ar/50 sccm H_2	1 sccm C_2H_2	50 sccm	50.00	Ar	20 sccm Ar	no	no	1.1 nm Fe + 10~20 nm Al_2O_3	650 °C	hot wall reactor				
Roberton	25	10-60 min	0.1-0.5 mbar	10% C_2H_2	0.1-0.5 mbar NH3		no	no	no	no	1 nm Fe + 15 nm CoSi2+ 200 nm poly-Si	650 °C	low pressure cold wall	90 min			
Roberton	25	90 min	150-250 mbar Ar:H_2	2% C_2H_2	150-250 mbar Ar:H_2		no	no	no	no	1 nm Fe + 15 nm CoSi2+ 200 nm poly-Si	650 °C	Near atmospheric pressure cold wall	30 min			
Roberton	25	3 min	1000 mbar Ar:H_2	2% C_2H_2	1000 mbar Ar:H_2		no	no	no	no	1 nm Fe + 15 nm CoSi2+ 200 nm poly-Si	650 °C	Atmospheric pressure hot wall reactor	30 min	<10 um		
Roberton	26	3 min	500 sccm H_2 /200 sccm Ar	10 sccm C_2H_2	500 sccm	50.00	Ar	200 sccm	no	no	1.1 nm Fe + 100 nm Ta	650 °C	Atmospheric pressure hot wall reactor				
Roberton	26	20 min	0.1 mbar H_2	2×10^{-2} mbar C_2H_2	no	0.00	no	no	no	no	1.1 nm Fe + 100 nm Ta	650 °C	Medium pressure cold wall	5-10 min			
Roberton	27	30 min	Ar/H_2 =30:10 sccm	1 sccm	10 sccm	10.00	Ar	30 sccm	no	no	0.5 nm or 1 nm Ni, Co, Fe+100 nm TiN + 200 nm SiO_2	650 °C	XPS chamber				
Roberton	30	15 min	200 sccm Ar/500 sccm H_2	10 sccm C_2H_2	500 sccm	50.00	Ar	200 sccm Ar	no	no	1 nm Fe+ 10 nm Al_2O_3 or 20 nm CoSi2	650 °C	hot wall reactor (2 inch diameter)	30 min			
Roberton	31	10 min	0.6 mbar NH3	1/5×0.7 mbar C_2H_2	4/5×0.7 mbar NH_3		no	no	no	no	colloidal palladium nanoparticles (mean particle diameter of 2.4 nm)+ mesoporous thin films	650 °C	plasma-enhanced chemical vapor deposition	50s-3 min			
Roberton	35	5 min	200 sccm H_2	5 sccm C_2H_2	195 sccm	39.00	no	no	no	no	0.5 nm Al+0.5-0.7 nm Fe+10 nm Al_2O_3	650 °C	hot wall	90 min	1400 um		
Roberton	35	5 min	200 sccm H_2	5 sccm C_2H_2	195 sccm	39.00	no	no	no	no	0.5 nm Al+0.5-0.7 nm Fe+10 nm Al_2O_3	650 °C	hot wall	10 min	200 um		

Group	Paper #	annea l time	anneal gas	C_xH_y flow	H_2 flow	H_2/ C_xH_y	carrier gas	carrier gas flow	growth enhancer (Y/N)	Growth enhancer	catalyst	Tem.	reactor	growth time	terminal length	yield	SWCNT or MWCNT
Roberton	36	15 min	200 sccm NH_3 (0.6 mbar)	50 sccm C_2H_2	200 sccm NH_3		no	no	no	no	stainless steel (317-2R) or stainless steel (317-2R) coated with cobalt colloid nanoparticles	650 °C	plasma-enhanced chemical vapor deposition	20 min	5 um		MWCNT
Roberton	43	3 min	200 sccm Ar/500 sccm H_2	10 sccm	500 sccm	50.00	Ar	200 sccm	no	no	1 nm Fe+10 nm Al_2O_3 + 200 nm SiO_2	650 °C	2 inch hot wall reactor	30 min	200 um		
Roberton	43	3 min	200 sccm Ar/500 sccm H_2	10 sccm	500 sccm	50.00	Ar	200 sccm	no	no	1 nm Fe+10 nm Al_2O_3 + 200 nm SiO_2	650 °C	2 inch hot wall reactor	30 min	400 um		
Milne	4			75 sccm	200 sccm NH_3						5 nm Ni + 20 nm SiO_2	650 °C	plasma-enhanced CVD		~4 um		MWCNT
Ajayan	14			15% of total flow	no	0.00	Ar	85% of total flow				650 °C	hot wall CVD				
Milne	22		700 sccm H_2 at 10 mbar	20 sccm	700 sccm	35.00					1 nm Fe + 10 nm Al_2O_3	655 °C	microheater	15 min			
Roberton	7	5 min	10^{-3} mbar vacuum	10 sccm, 0.1 mbar	no	0.00	no	no	no	no	1 nm Fe/ 0~130 nm Ta	670 °C	laser induced CVD , sport size 1 um	45 min			MWCNT
Roberton	7	5 min	100 sccm NH_3 at 1 mbar	10 sccm, 0.1 mbar	100 sccm NH_3 at 1mbar		no	no	no	no	1 nm Fe/ 0~130 nm Ta	670 °C	laser induced CVD, spot size 1 um	45 min			MWCNT
Milne	8			54 sccm	200 sccm NH_3						7 nm Ni + 15 nm TiN	675 °C	plasma-enhanced CVD				
Roberton	4	5 min	200 sccm Ar/500 sccm H_2	10 sccm	500 sccm	50.00	Ar	200 sccm	no	no	Ni/SiO_2 or Al_2O_3	700 °C	hot wall	5 min	350 um		
Roberton	4	5 min	200 sccm Ar/500 sccm H_2	50 sccm	200 sccm NH_3		no	no	no	no	Ni /SiO_2 or Al_2O_3	700 °C	plasma enhanced chemical vapor deposition	5 min			
Roberton	5	10 min at 600, 650, 700 °C	10^{-3} mbar H_2	10^{-2} mbar	no	0.00	no	no	no	no	0.5 nm, 1 nm, 2 nm, 3 nm, 4 nm, 5 nm Fe on TiN and poly-crystalline PtSi films	700 °C	cold wall	15 min			
Roberton	6		10^{-3} mbar NH_3	10^{-3} mbar C_2H_2	no	0.00	no	no	no	no	0.1 nm Co/200 nm SiO_2	700 °C	low pressure chemical vapor deposition (cold wall)	15 min			
Roberton	9	5 min	1000 sccm Ar + 500 sccm H_2	10 sccm C_2H_2	500 sccm	50.00	Ar	1000 sccm Ar	no	no	0.5, 1.0 or 5.0 nm Fe on 50 nm AlSi or 50 nm TiSiN or 50 nm TiN	700 °C	hot wall reactor	15 min	~200 um		MWCNT
Roberton	10	5 min	1000 sccm Ar + 500 sccm H_2	10 sccm C_2H_2	500 sccm	50.00	Ar	1000 sccm Ar	no	no	1 nm Fe/10 nm untreated or plasma-treated Al_2O_3	700 °C	hot wall reactor	10 min	1000 um		
Roberton	11	3 min	500 sccm H_2	40 sccm C_2H_2	460 sccm	11.50	no	no	no	no	(0.5-2 nm)Fe+10 nm Ti+(0-2 nm)Fe	700 °C	cold wall reactor	6 min or 10 min	<10 um		
Roberton	15	5 min	1000 sccm Ar + 500 sccm H_2	5, 8, 10, 15 sccm	500 sccm	50.00	Ar	1000 sccm Ar	no	no	0.5, 1.0, or 2.0 nm high purity Ni, Co, or Fe or a combination of two of them (in equal proportions) and same total thickness	700 °C	hot wall reactor	5, 10, 15 min			
Roberton	19	700 °C	1 mbar NH_3	20 mbar C_2H_2	no	0.00	no	no	no	no	1 nm Fe, Ni, Co on poly-Si	700 °C	cold wall reactor				
Roberton	23	5 min	15 mbar H_2; 500 sccm H_2	8% C_2H_2 at 15 mbar; 40 sccm C_2H_2	92% H_2 at 15 mbar; 460 sccm	11.50	no	no	no	no	0.5 nm Al/0.3 or 0.4 nm Fe/5 nm Al/Si (100)	700 °C	cold wall reactor	30 min	60 um at 625 °C , 20 nm Al_2O_3		SWCNT and DWCNT
Roberton	23	5 min	15 mbar H_2; 500 sccm H_2	1% C_2H_2 at 15 mbar; 5 sccm C_2H_2	99 % H_2 at 15 mbar; 495 sccm	99.00	no	no	no	no	0.5 nm Al/0.7 nm Fe/5 nm Al/Si (100)	700 °C	cold wall reactor				

Group	Paper #	annea l time	anneal gas	C_xH_y flow	H_2 flow	H_2/ C_xH_y	carrier gas	carrier gas flow	growth enhancer (Y/N)	Growth enhancer	catalyst	Tem.	reactor	growth time	terminal length	yield	SWCNT or MWCNT
Roberton	23	5 min	15 mbar H_2; 500 sccm H_2	2 % C_2H_2 at 15 mbar; 10 sccm C_2H_2	98 % H_2 at 15 mbar; 490 sccm	49.00	no	no	no	no	0.5 nm Al/0.4 or 0.9 nm Fe/5 nm Al/Si (100)	700 °C	cold wall reactor				
Roberton	23	5 min	15 mbar H_2; 500 sccm H_2	4 % C_2H_2 at 15 mbar; 20 sccm C_2H_2	96 % H_2 at 15 mbar; 480 sccm	24.00	no	no	no	no	0.5 nm Al/0.4 or 0.9 nm Fe/5 nm Al/Si (100)	700 °C	cold wall reactor				
Roberton	23	5 min	15 mbar H_2; 500 sccm H_2	6 % C2H2 at 15 mbar; 30 sccm C_2H_2	94 % H_2 at 15 mbar; 470 sccm	15.67	no	no	no	no	0.5 nm Al/0.4 or 0.9 nm Fe/5 nm Al/Si (100)	700 °C	cold wall reactor				
Roberton	23	5 min	15 mbar H_2; 500 sccm H_2	8 % C_2H_2 at 15 mbar; 40 sccm C_2H_2	92 % H_2 at 15 mbar; 460 sccm	11.50	no	no	no	no	0.5 nm Al/0.4 or 0.9 nm Fe/5 nm Al/Si (100)	700 °C	cold wall reactor				
Roberton	23	5 min	15 mbar H_2; 500 sccm H_2	10 % C_2H_2 at 15 mbar; 50 sccm C_2H_2	90 % H_2 at 15 mbar; 450 sccm	9.00	no	no	no	no	0.5 nm Al/0.4 or 0.9 nm Fe/5 nm Al/Si (100)	700 °C	cold wall reactor				
Roberton	26	3 min	500 sccm H_2 /200 sccm Ar	10 sccm C_2H_2	500 sccm	50.00	Ar	200 sccm	no	no	1.1 nm Fe + 100 nm Ta	700 °C	Atmospheric pressure hot wall reactor				
Roberton	26	40 min	150 mbar H_2 /Ar (10:30)	1/41×15 0 mbar	10/41×1 50 mbar	10.00	Ar	30/41×15 0 mbar	no	no	4 nm Fe + 100 nm Ta	700 °C	Reduced pressure cold wall reactor	40 min			
Roberton	33	5 min	NH_3	10^{-5} mbar C_2H_2	no	0.00	no	no	no	no	0.5-1nm Fe+10 nm Al_2O_3 +200 nm thermal SiO_2	700 °C	UHV cold wall	5 min			
Roberton	33	5 min	NH_3	2.5×10^{-3} mbar C_2H_2	no	0.00	no	no	no	no	0.5-1nm Fe+10 nm Al_2O_3 +200 nm thermal SiO_2	700 °C	UHV pressure cold wall	5 min			
Roberton	37			1/5 C_2H_2	4/5 NH_3		no	no	no	no	7 nm Ni + 15 nm TiN	700 °C	plasma enhanced chemical vapor deposition	1-5 h			SWCNT
Roberton	43	3 min	200 sccm Ar/500 sccm H_2	10 sccm	500 sccm	50.00	Ar	200 sccm	no	no	1 nm Fe+10 nm Al_2O_3 + 200 nm SiO_2	700 °C	2 inch hot wall reactor	30 min	750 um		
Hata	20			5 mL/min	30 mL/min	6.00	Ar	120 mL/min	no	no	iron on Si	700 °C	hot wall reactor				SWCNT
Hata	23			5 sccm	30 sccm	6.00	Ar	120 sccm	no	no	FePt nanoparticle	700 °C	thermal CVD reactor		exceeding 100 um		SWCNT
Homma	27		100 sccm Ar/H_2 (3% H_2 by volume)	0.5% ×300 sccm	700 sccm×3 %	6.00	Ar	300×99.5 %+700×9 7%	no	no	crystalline iron oxide nanoparticles dispersed in toluene depositing on Al_2O_3 by spin coating method	700 °C	atmospheric pressure CVD				
Milne	1				NH_3 was used						3 nm Ni + SiO_2	700 °C	plasma-enhanced CVD		~4 um		MWCNT
Milne	2				NH_3 was used						3 nm Ni + SiO_2	700 °C	plasma-enhanced CVD	growth time was chosen to obtain CNTs up to ~0.4 um heights	~0.4 um		MWCNT
Milne	3				NH_3 was used						3 nm Ni + 20 nm TiN	700 °C	plasma-enhanced CVD				MWCNT

Group	Paper #	annea l time	anneal gas	C_xH_y flow	H_2 flow	H_2/ C_xH_y	carrier gas	carrier gas flow	growth enhancer (Y/N)	Growth enhancer	catalyst	Tem.	reactor	growth time	terminal length	yield	SWCNT or MWCNT
Milne	5				NH_3 was used						3 nm Ni + SiO_2	700 °C	plasma-enhanced CVD				
Milne	7			40 sccm	200 sccm NH_3						3 nm Ni + 30 nm SiO_2	700 °C	plasma-enhanced CVD	15 min	5 um		
Milne	10	550 °C for 1 min	200 sccm NH_3	54 sccm	200 sccm NH_3						7 nm Ni + 15 nm indium tin oxide	700 °C	plasma-enhanced CVD				
Milne	11			4% to 20%	NH_3							700 °C	plasma-enhanced CVD	10 s			SWCNT
Milne	13			1/5 total gas	4/5×tota l flow NH_3							700 °C	plasma-enhanced CVD				
Milne	19				NH_3							700 °C	plasma enhanced CVD				
Milne	21		NH_3 or N_2	1/6×tota l flow	5/6×tota l flow NH_3							700 °C	plasma-enhanced CVD				
Milne	23	10 min	500 mbar NH_3				N_2		yes	water	4 nm Fe + 200 nm SiO_2	700 °C	hot filament CVD, vertical gas flow structure, hot filament temperature at 1000 °C is the best				
Milne	27			200 sccm	50 sccm NH_3						Ni or 1nm Fe/ 10 nm Al2Ox	700 °C	horizontal plasma-enhanced CVD				
Roberton	6	ramping up to 700 °C in 1 min, keep at 700 °C for 4 min	10^{-3} mbar NH_3 for C_2H_2 growth, 5 mbar NH_3 for ethanol growth	10^-3 mbar C_2H_2 or 5 mbar CH_3CH_2OH	no	0.00	no	no	no	no	0.1 nm Co/200 nm SiO_2	700 °C	low pressure chemical vapor deposition (cold wall)	15 min			SWCNT
Milne	12			100 sccm							0.3 nm Mo + 1 nm Fe + 10 nm Al +SiO_2	725 °C	cold wall reactor				
Milne	15				NH_3						5 nm Ni	725 °C	plasma-enhanced CVD				
Hata	27			0.4-2%			He		yes	water (20-900 ppm)	1.8 nm Fe+40 nm Al_2O_3	725 °C for plotting 725 °C to 825 °C	1 inch fully automated CVD system equiped with a telecentric optical system for in situ height measurements.				
Hata	27			0.4-2%			He		yes	water (20-900 ppm)	1.8 nm Fe+40 nm Al_2O_3	775 °C for plotting 725 °C to 825 °C	1 inch fully automated CVD system equiped with a telecentric optical system for in situ height measurements.				
Hata	25	750 °C	1:9 He/H_2	25 sccm C_2H_4			He	total flow 500 sccm	yes	water (50 to 500 ppm)	1.5 nm Fe + 40 nm Al_2O_3	725 °C for plotting 725 to 900 °C	1 inch fully automated CVD system				SWCNT
Hata	25	750 °C	1:9 He/H_2	25 sccm C_2H_4			He	total flow 500 sccm	yes	water (50 to 500 ppm)	1.5 nm Fe + 40 nm Al_2O_3	775 °C for plotting 725 to 900 °C	1 inch fully automated CVD system				
Hata	25	750 °C	1:9 He/H_2	25 sccm C_2H_4			He	total flow 500 sccm	yes	water (50 to 500 ppm)	1.5 nm Fe + 40 nm Al_2O_3	875 °C for plotting 725 to 900 °C	1 inch fully automated CVD system				
Milne	22		700 sccm H_2 at 10 mbar	20 sccm	700 sccm	35.00					1 nm Fe + 10 nm Al_2O_3	748 °C	microheater				
Roberton	4	5 min	500 sccm H_2	40 sccm	460 sccm	11.50	no	no	no	no	Fe/Al_2O_3 or SiO_2	750 °C	cold wall CVD chamber with low pressure	5 min	100 um		DWCNT
Roberton	10	5 min	1000 sccm Ar + 500 sccm H_2	10 sccm C_2H_2	500 sccm	50.00	Ar	1000 sccm Ar	no	no	1 nm Fe/10 nm Al_2O_3	750 °C	hot wall reactor	10 min	300 um		

Group	Paper #	annea l time	anneal gas	C_xH_y flow	H_2 flow	H_2/ C_xH_y	carrier gas	carrier gas flow	growth enhancer (Y/N)	Growth enhancer	catalyst	Tem.	reactor	growth time	terminal length	yield	SWCNT or MWCNT
Roberton	10	5 min	1000 sccm Ar + 500 sccm H_2	10 sccm C_2H_2	500 sccm	50.00	Ar	1000 sccm Ar	no	no	1 nm Fe/10 nm plasma treated Al_2O_3	750 °C	hot wall reactor	10 min	1000 um		
Roberton	10	5 min	1000 sccm Ar + 500 sccm H_2	5 sccm C_2H_2	500 sccm	100.0 0	Ar	1000 sccm Ar	no	no	0.5 nm Fe/10 nm Al_2O_3	750 °C	hot wall reactor	60 min	200 um		
Roberton	10	5 min	1000 sccm Ar + 500 sccm H_2	5 sccm C_2H_2	500 sccm	100.0 0	Ar	1000 sccm Ar	no	no	0.5 nm Fe/10 nm plasma treated Al_2O_3	750 °C	hot wall reactor	60 min	2000 um		
Roberton	12	3 min	500 sccm H_2 /200 sccm Ar	10 sccm C_2H_2	500 sccm	50.00	Ar	20 sccm Ar	no	no	0.5 nm Ta-oxide/SiO_2	750 °C	hot wall reactor				
Roberton	12	3 min	500 sccm H_2 /200 sccm Ar	10 sccm C_2H_2	500 sccm	50.00	Ar	20 sccm Ar	no	no	0.7 nm Ta-oxide/SiO_2	750 °C	hot wall reactor				
Roberton	12			1/11×0.5 mbar	10/11×0.5 mbar	10.00	no	no	no	no	0.5 nm Ta-oxide/SiO_2	750 °C	low pressure CVD				
Roberton	12			0.5 mbar	no	0.00	no	no	no	no	0.5 nm Ta-oxide/SiO_2	750 °C	low pressure CVD				
Roberton	15	5 min	1000 sccm Ar + 500 sccm H_2	5, 8, 10, 15 sccm	500 sccm	50.00	Ar	1000 sccm Ar	no	no	0.5, 1.0, or 2.0 nm high purity Ni, Co, or Fe or a combination of two of them (in equal proportions) and same total thickness	750 °C	hot wall reactor	5, 10, 15 min			
Roberton	19	750 °C	1 mbar NH_3	20 mbar C_2H_2	no	0.00	no	no	no	no	1 nm Fe, Ni, Co on momo-Si	750 °C	cold wall reactor				
Roberton	21		30 sccm Ar/ 10 sccm H_2	1 sccm C_2H_2	10 sccm	10.00	Ar	30 sccm	no	no	8 nm Fe + 10 nm Al_2O_3	750 °C	cold wall reactor	5 min			MWCNT
Roberton	24	3 min	20 sccm Ar/50 sccm H_2	1 sccm C_2H_2	50 sccm	50.00	Ar	20 sccm Ar	no	no	1.1 nm Fe + 10~20 nm Al_2O_3	750 °C	hot wall reactor				
Roberton	26	3 min	500 sccm H_2 /200 sccm Ar	10 sccm C_2H_2	500 sccm	50.00	Ar	200 sccm	no	no	1.1 nm Fe + 100 nm Ta	750 °C	Atmospheric pressure hot wall reactor				
Roberton	28	ramping up to 500 °C to 750 °C	1000 sccm Ar + 500 sccm H_2	10 sccm C_2H_2	500 sccm	50.00	Ar	1000 sccm Ar	no	no	0.1 to 0.5 nm Fe, Co, or Ni + 10 nm Al_2O_3 +200 nm SiO_2	750 °C	hot wall reactor	1 min			
Roberton	33			10 sccm C_2H_2	500 sccm	50.00	Ar	200 sccm Ar	no	no	0.5-1nm Fe+10 nm Al_2O_3 +200 nm thermal SiO_2	750 °C	2 inch hot wall reactor				
Roberton	39		Ar+H_2	10 sccm C_2H_2	500 sccm	50.00	Ar	200 sccm Ar	no	no	0.9 nm Fe+10 nm Al_2O_3 or SiO_2	750 °C	2 inch hot wall reactor				
Roberton	43	3 min	200 sccm Ar/500 sccm H_2	10 sccm	500 sccm	50.00	Ar	200 sccm	no	no	1 nm Fe+10 nm Al_2O_3 + 200 nm SiO_2	750 °C	2 inch hot wall reactor	30 min	0 um		
Roberton	43	3 min	200 sccm Ar/500 sccm H_2	5 sccm	500 sccm	100.0 0	Ar	200 sccm	no	no	1 nm Fe+10 nm Al_2O_3 + 200 nm SiO_2	750 °C	2 inch hot wall reactor	30 min	0 um		
Roberton	43	3 min	200 sccm Ar/500 sccm H_2	55 sccm	500 sccm	9.09	Ar	200 sccm	no	no	1 nm Fe+10 nm Al_2O_3 + 200 nm SiO_2	750 °C	2 inch hot wall reactor	60 min	1200 um		
Roberton	43	3 min	200 sccm Ar/500 sccm H_2	10 sccm	500 sccm	50.00	Ar	200 sccm	no	no	1 nm Fe+10 nm Al_2O_3 + 200 nm SiO_2	750 °C	2 inch hot wall reactor	180 min	1750 um		
Roberton	43	3 min	200 sccm Ar/500 sccm H_2	10 sccm	500 sccm	50.00	Ar	200 sccm	no	no	1 nm Fe+10 nm Al_2O_3 + 200 nm SiO_2	750 °C	2 inch hot wall reactor	10 min			MWCNT
Roberton	44			30 sccm C_2H_2	2000 sccm	66.67	N_2	800 sccm N_2	no	no	Ni nanoparticles on Si	750 °C	4 inch hot wall				
Milne	12			100 sccm							0.3 nm Mo + 1 nm Fe + 10 nm Al +SiO_2	750 °C	cold wall reactor				
Homma	31											750 °C	cold wall CVD in the chamber of SEM		~5 um		MWCNT
Roberton	1	ramping from room temperature to 680 °C	500 sccm H_2	1-8% ×500 sccm	(99-92)%×500	24.00	no	no	no		0.4-1.0nmFe/5-20nm AlO_x	760 °C	cold wall reactor	tens seconds to a few minutes			SWCNT
Roberton	1	1.5 min	500 sccm H_2	2% ×500 sccm	98%×500	49.00	no	no	no	no	0.4nm Fe/6 nm AlO_x	760 °C	cold wall reactor	0.5 min	9.2 um		SWCNT

Group	Paper #	annea l time	anneal gas	C_xH_y flow	H_2 flow	H_2/ C_xH_y	carrier gas	carrier gas flow	growth enhancer (Y/N)	Growth enhancer	catalyst	Tem.	reactor	growth time	terminal length	yield	SWCNT or MWCNT
Roberton	1	1.5 min	500 sccm H_2	2%×500 sccm	98%×500 sccm	49.00	no	no	no	no	1nmFe/6nmAlO$_x$	760 °C	cold wall reactor	0.5 min			MWCNT
Milne	22		700 sccm H_2 at 10 mbar	20 sccm	700 sccm	35.00					1 nm Fe + 10 nm Al_2O_3	773 °C	microheater				
Hata	13			30-50 sccm			He+H_2	1000 sccm	yes	water (100-200 ppm)	1.6-5 nm Fe on 40 nm Al_2O_3	790 °C for plotting (780 °C to 810 °C)	3 inch tube furnace				
Milne	22		700 sccm H_2 at 10 mbar	20 sccm	700 sccm	35.00					1 nm Fe + 10 nm Al_2O_3	794 °C	microheater				
Roberton	33			10 sccm C_2H_2	500 sccm	50.00	Ar	200 sccm Ar	no	no	0.5-1nm Fe+10 nm Al_2O_3 +200 nm thermal SiO_2	800 °C	2 inch hot wall reactor				
Roberton	43	3 min	200 sccm Ar/500 sccm H_2	10 sccm	500 sccm	50.00	Ar	200 sccm	no	no	1 nm Fe+10 nm Al_2O_3 + 200 nm SiO_2	800 °C	2 inch hot wall reactor	30 min	100 um		
Hata	18			100 sccm to 900 sccm, 10% of total gas flow			He+H_2	total gas flow from 1000 to 9000 sccm	yes	water	1 nm Fe+10 nm Al_2O_3	800 °C	3 in. infrared-heated vertical furnace with a long heating length (265 mm)	10 min			SWNT
Milne	12			100 sccm							0.3 nm Mo + 1 nm Fe + 10 nm Al +SiO_2	800 °C	cold wall reactor				
Hata	28			1-4 ×10^{-5}, peak at 2.4×10^{-5} mol/cm 2/min					yes	water	1.8 nm Fe+40 nm Al_2O_3	810 °C	hot wall CVD	10 min			
Milne	12			100 sccm							0.3 nm Mo + 1 nm Fe + 10 nm Al +SiO_2	830 °C	cold wall reactor				
Roberton	12	3 min	500 sccm H_2 /200 sccm Ar	10 sccm C_2H_2	500 sccm	50.00	Ar	20 sccm Ar	no	no	0.2 to 2.0 nm Ta-oxide/SiO_2	850 °C	hot wall reactor				
Roberton	12	3 min	500 sccm H_2 /200 sccm Ar	10 sccm C_2H_2	500 sccm	50.00	Ar	20 sccm Ar	no	no	0.2 to 2.0 nm Ta-oxide/Al_2O_3	850 °C	hot wall reactor				
Homma	26	15 min	100 sccm Ar/H_2 (3% H_2 by volume) at 700 Torr	0.1-0.4%×300 sccm	no	0.00	Ar	99.6-99.9% ×300 sccm	no	no	0.3 nm Fe or Co + 10 nm Al_2O_3	850 °C	horizontal quartz furnace	30 min			
Milne	12			100 sccm							0.3 nm Mo + 1 nm Fe + 10 nm Al +SiO_2	860 °C	cold wall reactor	20 min	~5 um		MWCNT
Milne	12			100 sccm							0.3 nm Mo + 1 nm Fe + 10 nm Al +SiO_2	900 °C	cold wall reactor				
Hata	24			10% diluted with He													
Roberton	8		200 sccm NH_3	200 sccm C_2H_2	no	0.00	no	no	no	no							
Roberton	8		200 sccm H_2	200 sccm C_2H_2	no	0.00	no	no	no	no							
Roberton	8		180 sccm NH_3+ 20 sccm Ar	20 sccm C_2H_2	180 sccm NH_3		no	no	no	no							
Roberton	8		180 sccm H_2 + 20 sccm Ar	20 sccm C_2H_2	180 sccm	9.00	no	no	no	no							
Roberton	39						no	no	no	no	Fe+10 nm Al_2O_3 +200 nm SiO_2 +Si (100)		high vacuum, in the mbar range, and at atmospheric pressure	5 min			

	Paper Number	Journal	year	Title
Roberton, J. at University of Cambridge	1	Carbon	2016	Growth of high quality, high density single-walled carbon nanotube forests on copper foils
Roberton, J. at University of Cambridge	2	Journal of Applied Physics	2015	The synergistic effect in the Fe-Co bimetallic catalyst system for the growth of carbon nanotube forests
Roberton, J. at University of Cambridge	3	ACS Applied Materials & Interfaces	2015	Low-Temperature Growth of Carbon Nanotube Forests Consisting of Tubes with Narrow Inner Spacing Using Co/Al/Mo Catalyst on Conductive Supports
Roberton, J. at University of Cambridge	4	Journal of Applied Physics	2014	Carbon nanotube forests growth using catalysts from atomic layer deposition
Roberton, J. at University of Cambridge	5	Carbon	2014	Carbon nanotube growth on conductors: Influence of the support structure and catalyst thickness
Roberton, J. at University of Cambridge	6	Journal of Physical Chemistry C	2014	Effect of Catalyst Pretreatment on Chirality-Selective Growth of Single-Walled Carbon Nanotubes
Roberton, J. at University of Cambridge	7	ACS Applied Materials & Interfaces	2014	Co-catalytic Absorption Layers for Controlled Laser-Induced Chemical Vapor Deposition of Carbon Nanotubes
Roberton, J. at University of Cambridge	8	ACS Applied Materials & Interfaces	2014	Growth Kinetics and Growth Mechanism of Ultrahigh Mass Density Carbon Nanotube Forests on Conductive Ti/Cu Supports
Roberton, J. at University of Cambridge	9	Physica Status Solidi B-Basic Solid State Physics	2014	Comparison of carbon nanotube forest growth using AlSi, TiSiN, and TiN as conductive catalyst supports
Roberton, J. at University of Cambridge	10	Journal of Physical Chemistry C	2014	Effect of Oxygen Plasma Alumina Treatment on Growth of Carbon Nanotube Forests
Roberton, J. at University of Cambridge	11	Carbon	2014	Single-step CVD growth of high-density carbon nanotube forests on metallic Ti coatings through catalyst engineering
Roberton, J. at University of Cambridge	12	RSC Advances	2013	Tantalum-oxide catalysed chemical vapour deposition of single- and multi-walled carbon nanotubes
Roberton, J. at University of Cambridge	13	Microelectronic Engineering	2013	Synthesis of carbon nanotubes and graphene for VLSI interconnects
Roberton, J. at University of Cambridge	14	Applied Physics Letters	2013	Low temperature growth of ultra-high mass density carbon nanotube forests on conductive supports
Roberton, J. at University of Cambridge	15	Physica Status Solidi B-Basic Solid State Physics	2013	Evaluation of bimetallic catalysts for the growth of carbon nanotube forests
Roberton, J. at University of Cambridge	16	Nanotechnology	2013	Carbon nanotube growth for through silicon via application
Roberton, J. at University of Cambridge	17	Carbon	2013	High density carbon nanotube growth using a plasma pretreated catalyst
Roberton, J. at University of Cambridge	18	Journal of Physical Chemistry C	2012	Co-Catalytic Solid-State Reduction Applied to Carbon Nanotube Growth
Roberton, J. at University of Cambridge	19	Journal of Applied Physics	2012	Plasma stabilisation of metallic nanoparticles on silicon for the growth of carbon nanotubes
Roberton, J. at University of Cambridge	20	Physica Status Solidi B-Basic Solid State Physics		Chemical vapor deposition of carbon nanotube forests
Roberton, J. at University of Cambridge	21	Chemistry of Materials	2012	The Phase of Iron Catalyst Nanoparticles during Carbon Nanotube Growth
Roberton, J. at University of Cambridge	22	Journal of Applied Physics	2012	Complementary metal-oxide-semiconductor-compatible and self-aligned catalyst formation for carbon nanotube synthesis and interconnect fabrication
Roberton, J. at University of Cambridge	23	Acs Nano	2012	Growth of Ultrahigh Density Single-Walled Carbon Nanotube Forests by Improved Catalyst Design
Roberton, J. at University of Cambridge	24	Thin Solid Films	2011	Carbon nanotube forest growth on NiTi shape memory alloy thin films for thermal actuation
Roberton, J. at University of Cambridge	25	Journal of Applied Physics	2011	In-situ study of growth of carbon nanotube forests on conductive CoSi2 support
Roberton, J. at University of Cambridge	26	Journal of Physical Chemistry C	2011	Support-Catalyst-Gas Interactions during Carbon Nanotube Growth on Metallic Ta Films
Roberton, J. at University of Cambridge	27	Journal of Applied Physics	2011	Use of plasma treatment to grow carbon nanotube forests on TiN substrate
Roberton, J. at University of Cambridge	28	Acs Nano	2010	Growth of Ultrahigh Density Vertically Aligned Carbon Nanotube Forests for Interconnects
Roberton, J. at University of Cambridge	29	Physica Status Solidi B-Basic Solid State Physics	2010	High-density growth of horizontally aligned carbon nanotubes for interconnects
Roberton, J. at University of Cambridge	30	Journal of Applied Physics	2010	Growth of vertically-aligned carbon nanotube forests on conductive cobalt disilicide support
Roberton, J. at University of Cambridge	31	Journal of Materials Science	2009	Confined palladium colloids in mesoporous frameworks for carbon nanotube growth
Roberton, J. at University of Cambridge	32	Journal of Physical Chemistry C	2009	State of Transition Metal Catalysts During Carbon Nanotube Growth
Roberton, J. at University of Cambridge	33	Acs Nano	2009	Diffusion- and Reaction-Limited Growth of Carbon Nanotube Forests
Roberton, J. at University of Cambridge	34	Diamond and Related Materials	2009	State of the catalyst during carbon nanotube growth
Roberton, J. at University of Cambridge	35	Journal of Physical Chemistry C	2009	Acetylene: A Key Growth Precursor for Single-Walled Carbon Nanotube Forests
Roberton, J. at University of Cambridge	36	Diamond and Related Materials	2008	Catalytic growth of carbon nanotubes on stainless steel: Characterization and frictional properties
Roberton, J. at University of Cambridge	37	Nanotechnology	2008	Carbon nanotube based photathodes
Roberton, J. at University of Cambridge	38	Nano Letters	2008	Mechanism analysis of interrupted growth of single-walled carbon nanotube arrays
Roberton, J. at University of Cambridge	39	Journal of Physical Chemistry C	2008	In-situ X-ray photoelectron spectroscopy study of catalyst-support interactions and growth of carbon nanotube forests
Roberton, J. at University of Cambridge	40	Physica E-Low-Dimensional Systems & Nanostructures	2008	Surface-bound chemical vapour deposition of carbon nanotubes: In situ study of catalyst activation
Roberton, J. at University of Cambridge	41	Journal of Nanoscience and Nanotechnology	2008	Controlling the Catalyst During Carbon Nanotube Growth
Roberton, J. at University of Cambridge	42	Applied Physics Letters	2008	Growth and characterization of high-density mats of single-walled carbon nanotubes for interconnects
Roberton, J. at University of Cambridge	43	Diamond and Related Materials	2008	Growth of aligned millimeter-long carbon nanotube by chemical vapor deposition
Roberton, J. at University of Cambridge	44	Physica Status Solidi B-Basic Solid State Physics	2008	Growth of carbon nanotubes as horizontal interconnects
Roberton, J. at University of Cambridge	45	Nano Letters	2007	In situ observations of catalyst dynamics during surface-bound carbon nanotube nucleation
Roberton, J. at University of Cambridge	46	Journal of Micromechanics and Microengineering	2007	Synthesis of individual single-walled carbon nanotube bridges controlled by support micromachining
Roberton, J. at University of Cambridge	47	Journal of Physical Chemistry C	2007	Flying and crawling modes during surface-bound single wall carbon nanotube growth
Roberton, J. at University of Cambridge	48	Physica E-Low-Dimensional Systems & Nanostructures	2007	The role of precursor gases on the surface restructuring of catalyst films during carbon nanotube growth

	Paper Number	Journal	year	Title
University of Cambridge Roberton, J. at				
University of Cambridge Roberton, J. at	50	Journal of Applied Physics	2005	Effects of catalyst film thickness on plasma-enhanced carbon nanotube growth
University of Cambridge Roberton, J. at	51	Diamond and Related Materials	2004	Low-temperature plasma enhanced chemical vapour deposition of carbon nanotubes
University of Cambridge Roberton, J. at	52	Applied Physics Letters	2003	Direct growth of aligned carbon nanotube field emitter arrays onto plastic substrates
University of Cambridge Roberton, J. at	53	Journal of the Mechanics and Physics of Solids	2003	Determination of mechanical properties of carbon nanotubes and vertically aligned carbon nanotube forests using nanoindentation
Tsinghua University Zhang, Q & Wei, F at	1	Carbon	2015	Rational recipe for bulk growth of graphene/carbon nanotube hybrids: New insights from in-situ characterization on working catalysts
Tsinghua University Zhang, Q & Wei, F at	2	Advanced Materials	2014	Nitrogen-Doped Aligned Carbon Nanotube/Graphene Sandwiches: Facile Catalytic Growth on Bifunctional Natural Catalysts and Their Applications as Scaffolds for High-Rate Lithium-Sulfur Batteries
Tsinghua University Zhang, Q & Wei, F at	3	Small	2014	Nitrogen-Doped Graphene/Carbon Nanotube Hybrids: In Situ Formation on Bifunctional Catalysts and Their Superior Electrocatalytic Activity for Oxygen Evolution/Reduction Reaction
Tsinghua University Zhang, Q & Wei, F at	4	Carbon	2014	Controllable bulk growth of few-layer graphene/single-walled carbon nanotube hybrids containing Fe@C nanoparticles in a fluidized bed reactor
Tsinghua University Zhang, Q & Wei, F at	5	Advanced Materials	2014	Hierarchical Vine-Tree-Like Carbon Nanotube Architectures: In-Situ CVD Self-Assembly and Their Use as Robust Scaffolds for Lithium-Sulfur Batteries
Tsinghua University Zhang, Q & Wei, F at	6	Journal of Energy Chemistry	2013	Highly selective synthesis of single-walled carbon nanotubes from methane in a coupled Downer-turbulent fluidized-bed reactor
Tsinghua University Zhang, Q & Wei, F at	7	Small	2013	The Road for Nanomaterials Industry: A Review of Carbon Nanotube Production, Post-Treatment, and Bulk Applications for Composites and Energy Storage
Tsinghua University Zhang, Q & Wei, F at	8	Carbon	2013	The reason for the low density of horizontally aligned ultralong carbon nanotube arrays
Tsinghua University Zhang, Q & Wei, F at	9	Carbon	2013	Towards high purity graphene/single-walled carbon nanotube hybrids with improved electrochemical capacitive performance
Tsinghua University Zhang, Q & Wei, F at	10	Chinese Science Bulletin	2012	A review of the large-scale production of carbon nanotubes: The practice of nanoscale process engineering
Tsinghua University Zhang, Q & Wei, F at	11	Carbon	2012	Self-organization of nitrogen-doped carbon nanotubes into double-helix structures
Tsinghua University Zhang, Q & Wei, F at	12	ACS Nano	2012	Graphene/Single-Walled Carbon Nanotube Hybrids: One-Step Catalytic Growth and Applications for High-Rate Li-S Batteries
Tsinghua University Zhang, Q & Wei, F at	13	Nanoscale	2012	Preferential growth of short aligned, metallic-rich single-walled carbon nanotubes from perpendicular layered double hydroxide film
Tsinghua University Zhang, Q & Wei, F at	14	Chemsuschem	2011	Carbon Nanotube Mass Production: Principles and Processes
Tsinghua University Zhang, Q & Wei, F at	15	Applied Clay Science	2011	Improvement of oil adsorption performance by a sponge-like natural vermiculite-carbon nanotube hybrid
Tsinghua University Zhang, Q & Wei, F at	16	Advanced Materials	2010	A Three-Dimensional Carbon Nanotube/Graphene Sandwich and Its Application as Electrode in Supercapacitors
Tsinghua University Zhang, Q & Wei, F at	17	Nanoscale	2010	Patterning of hydrophobic three-dimensional carbon nanotube architectures by a pattern transfer approach
Tsinghua University Zhang, Q & Wei, F at	18	Applied Physics a-Materials Science & Processing	2010	Coupled process of plastics pyrolysis and chemical vapor deposition for controllable synthesis of vertically aligned carbon nanotube arrays
Tsinghua University Zhang, Q & Wei, F at	19	New Carbon Materials	2010	Growth of super long vertically aligned carbon nanotube arrays from cyclohexane via floating catalyst method
Tsinghua University Zhang, Q & Wei, F at	20	Angewandte Chemie-International Edition	2010	Carbon-Nanotube-Array Double Helices
Tsinghua University Zhang, Q & Wei, F at	21	Powder Technology	2010	Comparison of vertically aligned carbon nanotube array intercalated production among vermiculites in fixed and fluidized bed reactors
Tsinghua University Zhang, Q & Wei, F at	22	Carbon	2010	Dry spinning yarns from vertically aligned carbon nanotube arrays produced by an improved floating catalyst chemical vapor deposition method
Tsinghua University Zhang, Q & Wei, F at	23	Carbon	2010	Mass production of aligned carbon nanotube arrays by fluidized bed catalytic chemical vapor deposition
Tsinghua University Zhang, Q & Wei, F at	24	Journal of Physics and Chemistry of Solids	2010	Large scale intercalated growth of short aligned carbon nanotubes among vermiculite layers in a fluidized bed reactor
Tsinghua University Zhang, Q & Wei, F at	25	Powder Technology	2010	Hydrothermal mass production of $MgBO_2(OH)$ nanowhiskers and subsequent thermal conversion to $Mg_2B_2O_5$ nanorods for biaxially oriented polypropylene resins reinforcement
Tsinghua University Zhang, Q & Wei, F at	26	Nano Research	2009	Process Intensification by CO_2 for High Quality Carbon Nanotube Forest Growth: Double-Walled Carbon Nanotube Convexity or Single-Walled Carbon Nanotube Bowls?
Tsinghua University Zhang, Q & Wei, F at	27	Materials Letters	2009	Large area growth of aligned CNT arrays on spheres: Cost performance and product control
Tsinghua University Zhang, Q & Wei, F at	28	Applied Physics a-Materials Science & Processing	2009	Modulating the diameter of carbon nanotubes in array form via floating catalyst chemical vapor deposition
Tsinghua University Zhang, Q & Wei, F at	29	Journal of the Society for Information Display	2008	Growth of uniform carbon-nanotube arrays with sandwich technology
Tsinghua University Zhang, Q & Wei, F at	30	Carbon	2008	Liquefied petroleum gas containing sulfur as the carbon source for carbon nanotube forests
Tsinghua University Zhang, Q & Wei, F at	31	Powder Technology	2008	The mass production of carbon nanotubes using a nano-agglomerate fluidized bed reactor: A multiscale space-time analysis
Tsinghua University Zhang, Q & Wei, F at	32	Nano	2008	Few walled carbon nanotube production in large-scale by nano-agglomerate fluidized-bed process
Tsinghua University Zhang, Q & Wei, F at	33	Materials Chemistry and Physics	2008	In situ growth of carbon nanotubes on inorganic fibers with different surface properties
Tsinghua University Zhang, Q & Wei, F at	34	Carbon	2008	Radial growth of vertically aligned carbon nanotube arrays from ethylene on ceramic spheres
Tsinghua University Zhang, Q & Wei, F at	35	Chinese Journal of Catalysis	2008	Selective Synthesis of Single/Double/Multi-walled Carbon Nanotubes on MgO-Supported Fe Catalyst
Tsinghua University Zhang, Q & Wei, F at	36	AD'07: Proceedings of Asia Display 2007, Vols 1 and 2	2007	Growth of uniform Carbon Nanotube arrays with sandwich technology
Tsinghua University Zhang, Q & Wei, F at	37	Nanotechnology	2007	Large current carbon nanotube emitter growth using nickel as a buffer layer
Tsinghua University Zhang, Q & Wei, F at	38	Nanotechnology	2007	Ultrahigh-current field emission from sandwich-grown well-aligned uniform multi-walled carbon nanotube arrays with high adherence strength
Tsinghua University Zhang, Q & Wei, F at	39	Analyst	2007	Recent progress in chemical detection with single-walled carbon nanotube networks
Tsinghua University Zhang, Q & Wei, F at	40	New Carbon Materials	2007	Progress on aligned carbon nanotube arrays
Tsinghua University Zhang, Q & Wei, F at	41	Nanotechnology	2007	Temperature effect on the substrate selectivity of carbon nanotube growth in floating chemical vapor deposition
Tsinghua University Zhang, Q & Wei, F at	42	Small	2007	Advances in carbon-nanotube assembly
Tsinghua University Zhang, Q & Wei, F at	43	Chinese Science Bulletin	2007	Large scale production of carbon nanotube arrays on the sphere surface from liquefied petroleum gas at low cost
Tsinghua University Zhang, Q & Wei, F at	44	Journal of Physical Chemistry C	2007	Synchronous growth of vertically aligned carbon nanotubes with pristine stress in the heterogeneous catalysis process

	Paper Number	Journal	year	Title
Zhang, Q & Wei, F at Tsinghua University	45	Advanced Materials	2006	Field emission of electrons from single LaB6 nanowires
Zhang, Q & Wei, F at Tsinghua University	46	Surface & Coatings Technology	2003	Effects of oxygen and nitrogen on carbon nanotube growth using a microwave plasma chemical vapor deposition technique
Zhang, Q & Wei, F at Tsinghua University	47	Diamond and Related Materials	2001	Field emission from patterned carbon nanotube emitters produced by microwave plasma chemical vapor deposition
Hata, K at "Super Growth Group"	1	Science	2004	Water-Assisted Highly Efficient Synthesis of Impurity-Free Single-Walled Carbon Nanotubes
Hata, K at "Super Growth Group"	2	Journal of Physical Chemistry B	2005	Selective matching of catalyst element and carbon source in single-walled carbon nanotube synthesis on silicon substrates
Hata, K at "Super Growth Group"	3	Journal of Physical Chemistry B	2006	84% Catalyst activity of water-assisted growth of single walled carbon nanotube forest characterization by a statistical and macroscopic approach
Hata, K at "Super Growth Group"	4	Nature Nanotechnology	2006	Size-selective growth of double-walled carbon nanotube forests from engineered iron catalysts
Hata, K at "Super Growth Group"	5	Quantum Sensing and Nanophotonic Devices IV	2007	From highly efficient impurity-free CNT synthesis to DWNT forests, CNT solids and super-capacitors
Hata, K at "Super Growth Group"	6	Journal of Physical Chemistry C	2007	Water-assisted highly efficient synthesis of single-walled carbon nanotubes forests from colloidal nanoparticle catalysts
Hata, K at "Super Growth Group"	7	2007 Ieee 20th International Vacuum Nanoelectronics Conference	2007	Fabrication of field emitter by direct growth of carbon nanotube onto tungsten tip by chemical vapor deposition
Hata, K at "Super Growth Group"	8	Carbon Na Notubes: Advanced Topics in the Synthesis, Structure, Properties and Applications	2008	Carbon nanotube synthesis and organization
Hata, K at "Super Growth Group"	9	Nano Letters	2008	Revealing the Secret of Water-Assisted Carbon Nanotube Synthesis by Microscopic Observation of the Interaction of Water on the Catalysts
Hata, K at "Super Growth Group"	10	Applied Physics Letters	2008	Diagnostics and growth control of single-walled carbon nanotube forests using a telecentric optical system for in situ height monitoring
Hata, K at "Super Growth Group"	11	2009 Ieee Sensors, Vols 1-3	2009	Piezoresistive and Thermoelectric Effects of CNT Thin Film Patterned by EB Lithography
Hata, K at "Super Growth Group"	12	Acs Nano	2009	Improved and Large Area Single-Walled Carbon Nanotube Forest Growth by Controlling the Gas Flow Direction
Hata, K at "Super Growth Group"	13	Acs Nano	2009	Exploring Advantages of Diverse Carbon Nanotube Forests With Tailored Structures Synthesized by Supergrowth from Engineered Catalysts
Hata, K at "Super Growth Group"	14	Microelectronics Journal	2010	Integrated CNTs thin film for MEMS mechanical sensors
Hata, K at "Super Growth Group"	15	Smart Materials and Structures	2010	Integration of SWNT film into MEMS for a micro-thermoelectric device
Hata, K at "Super Growth Group"	16	Carbon	2011	Growth control of single-walled, double-walled, and triple-walled carbon nanotube forests by a priori electrical resistance measurement of catalyst films
Hata, K at "Super Growth Group"	17	Smart Materials & Structures	2011	The performance of fast-moving low-voltage electromechanical actuators based on single-walled carbon nanotubes and ionic liquids
Hata, K at "Super Growth Group"	18	Nano Letters	2011	Gas Dwell Time Control for Rapid and Long Lifetime Growth of Single-Walled Carbon Nanotube Forests
Hata, K at "Super Growth Group"	19	Journal of the American Chemical Society	2012	Role of Subsurface Diffusion and Ostwald Ripening in Catalyst Formation for Single-Walled Carbon Nanotube Forest Growth
Hata, K at "Super Growth Group"	20	Surface and Interface Analysis	2012	Effect of geometry of a vertically aligned carbon nanotube pillar array on its field-emission properties
Hata, K at "Super Growth Group"	21	Acs Nano	2013	Absence of an Ideal Single-Walled Carbon Nanotube Forest Structure for Thermal and Electrical Conductivities
Hata, K at "Super Growth Group"	22	Journal of Nanoscience and Nanotechnology	2013	Direct Wall Number Control of Carbon Nanotube Forests from Engineered Iron Catalysts
Hata, K at "Super Growth Group"	23	Vacuum	2013	Magnetic property of Fe Pt nanoparticles encaged in carbon nanotubes
Hata, K at "Super Growth Group"	24	Scientific Reports	2013	The Infinite Possible Growth Ambients that Support Single-Wall Carbon Nanotube Forest Growth
Hata, K at "Super Growth Group"	25	Acs Nano	2013	Unexpectedly High Yield Carbon Nanotube Synthesis from Low-Activity Carbon Feedstocks at High Concentrations
Hata, K at "Super Growth Group"	26	Materials	2013	A Fundamental Limitation of Small Diameter Single-Walled Carbon Nanotube Synthesis-A Scaling Rule of the Carbon Nanotube Yield with Catalyst Volume
Hata, K at "Super Growth Group"	27	Nanoscale	2015	The relationship between the growth rate and the lifetime in carbon nanotube synthesis
Hata, K at "Super Growth Group"	28	Nanomaterials	2015	The Application of Gas Dwell Time Control for Rapid Single Wall Carbon Nanotube Forest Synthesis to Acetylene Feedstock
Hata, K at "Super Growth Group"	28	Nanomaterials	2015	The Application of Gas Dwell Time Control for Rapid Single Wall Carbon Nanotube Forest Synthesis to Acetylene Feedstock
Hata, K at "Super Growth Group"	29	Nanoscale	2016	A phenomenological model for selective growth of semiconducting single-walled carbon nanotubes based on catalyst deactivation
Hart, A. John at MIT	1	Nano Letters	2006	Force output, control of film structure, and microscale shape transfer by carbon nanotube growth under mechanical pressure
Hart, A. John at MIT	2	Carbon	2006	Growth of conformal single-walled carbon nanotube films from Mo/Fe/Al_2O_3 deposited by electron beam evaporation
Hart, A. John at MIT	3	Journal of Physical Chemistry B	2006	Rapid growth and flow-mediated nucleation of millimeter-scale aligned carbon nanotube structures from a thin-film catalyst
Hart, A. John at MIT	4	Small	2007	Desktop growth of carbon-nanotube monoliths with in situ optical Imaging
Hart, A. John at MIT	5	Review of Scientific Instruments	2007	Suspended heated silicon platform for rapid thermal control of surface reactions with application to carbon nanotube synthesis
Hart, A. John at MIT	6	Journal of Physical Chemistry C	2007	Quantitative characterization of the morphology of multiwall carbon nanotube films by small-angle X-ray scattering
Hart, A. John at MIT	7	Applied Physics Letters	2008	Abrupt self-termination of vertically aligned carbon nanotube growth
Hart, A. John at MIT	8	Nano Letters	2008	Tuning of Vertically-Aligned Carbon Nanotube Diameter and Areal Density through Catalyst Pre-Treatment
Hart, A. John at MIT	9	Journal of Physical Chemistry C	2009	Collective Mechanism for the Evolution and Self-Termination of Vertically Aligned Carbon Nanotube Growth
Hart, A. John at MIT	10	Nanotechnology	2009	High-yield growth of vertically aligned carbon nanotubes on a continuously moving substrate
Hart, A. John at MIT	11	Acs Nano	2009	Engineering Vertically Aligned Carbon Nanotube Growth by Decoupled Thermal Treatment of Precursor and Catalyst
Hart, A. John at MIT	12	Nano Letters	2009	Low Temperature Synthesis of Vertically Aligned Carbon Nanotubes with Electrical Contact to Metallic Substrates Enabled by Thermal Decomposition of the Carbon Feedstock
Hart, A. John at MIT	13	Environmental Science & Technology	2009	Early Evaluation of Potential Environmental Impacts of Carbon Nanotube Synthesis by Chemical Vapor Deposition
Hart, A. John at MIT	14	Journal of the American Chemical Society	2009	Nanoscale Zirconia as a Nonmetallic Catalyst for Graphitization of Carbon and Growth of Single- and Multiwall Carbon Nanotubes
Hart, A. John at MIT	15	Small	2009	Flexible High-Conductivity Carbon-Nanotube Interconnects Made by Rolling and Printing
Hart, A. John at MIT	16	Nanoscale	2010	Measuring the lengthening kinetics of aligned nanostructures by spatiotemporal correlation of height and orientation
Hart, A. John at MIT	17	Acs Nano	2010	Multiple Alkynes React with Ethylene To Enhance Carbon Nanotube Synthesis, Suggesting a Polymerization-like Formation Mechanism
Hart, A. John at MIT				Fabrication and electrical integration of robust carbon nanotube micropillars by self-directed elastocapillary

	Paper Number	Journal	year	Title
				densification
Hart, A. John at MIT	19	Chemistry of Materials	2011	Multidirectional Hierarchical Nanocomposites Made by Carbon Nanotube Growth within Layer-by-Layer-Assembled Films
Hart, A. John at MIT	20	Carbon	2011	Precursor gas chemistry determines the crystallinity of carbon nanotubes synthesized at low temperature
Hart, A. John at MIT	21	Journal of Applied Physics	2011	Non-destructive characterization of structural hierarchy within aligned carbon nanotube assemblies
Hart, A. John at MIT	22	Carbon	2012	Diameter-dependent kinetics of activation and deactivation in carbon nanotube population growth
Hart, A. John at MIT	23	Acs Nano	2012	High-Speed in Situ X-ray Scattering of Carbon Nanotube Film Nucleation and Self-Organization
Hart, A. John at MIT	24	Advanced Functional Materials	2012	Wide Range Control of Microstructure and Mechanical Properties of Carbon Nanotube Forests: A Comparison Between Fixed and Floating Catalyst CVD Techniques
Hart, A. John at MIT	25	Nanoscale	2013	Mechanical coupling limits the density and quality of self-organized carbon nanotube growth
Hart, A. John at MIT	26	Review of Scientific Instruments	2013	Robofurnace: A semi-automated laboratory chemical vapor deposition system for high-throughput nanomaterial synthesis and process discovery
Hart, A. John at MIT	27	Acs Nano	2013	Statistical Analysis of Variation in Laboratory Growth of Carbon Nanotube Forests and Recommendations for Improved Consistency
Hart, A. John at MIT	28	Small	2013	Decoupled Control of Carbon Nanotube Forest Density and Diameter by Continuous-Feed Convective Assembly of Catalyst Particles
Hart, A. John at MIT	29	Acs Applied Materials & Interfaces	2013	Laser Printing of Nanoparticle Toner Enables Digital Control of Micropatterned Carbon Nanotube Growth
Hart, A. John at MIT	30	Acs Nano	2014	Synergetic Chemical Coupling Controls the Uniformity of Carbon Nanotube Microstructure Growth
Homma, Yoshikazu	1	Applied Physics Letters	2002	Growth of suspended carbon nanotube networks on 100-nm-scale silicon pillars
Homma, Yoshikazu	2	Japanese Journal of Applied Physics Part 2-Letters & Express Letters	2002	Single-walled carbon nanotube growth on silicon substrates using nanoparticle catalysts
Homma, Yoshikazu	3	Journal of Physical Chemistry B	2003	Role of transition metal catalysts in single-walled carbon nanotube growth in chemical vapor deposition
Homma, Yoshikazu	4	Journal of Physical Chemistry B	2003	High-density, large-area single-walled carbon nanotube networks on nanoscale patterned substrates
Homma, Yoshikazu	5	Thin Solid Films	2004	CVD growth of single-walled carbon nanotubes using size-controlled nanoparticle catalyst
Homma, Yoshikazu	6	Physica E-Low-Dimensional Systems & Nanostructures	2004	Surface and interface reactions of catalysts for carbon nanotube growth on Si substrates studied by soft X-ray photoelectron spectroscopy
Homma, Yoshikazu	7	Japanese Journal of Applied Physics Part 1-Regular Papers Brief Communications & Review Papers	2005	Bridging growth of single-walled carbon nanotubes on nanostructures by low-pressure hot-filament chemical vapor deposition
Homma, Yoshikazu	8	Chemical Physics Letters	2006	Behavior of catalytic nanoparticles during chemical vapor deposition for carbon nanotube growth
Homma, Yoshikazu	9	Surface and Interface Analysis	2006	In situ scanning electron microscopy of single-walled carbon nanotube growth
Homma, Yoshikazu	10	Nano Letters	2006	Single-walled carbon nanotube growth from highly activated metal nanoparticles
Homma, Yoshikazu	11	Japanese Journal of Applied Physics Part 1-Regular Papers Brief Communications & Review Papers	2007	Direct growth of vertically aligned single-walled carbon nanotubes on metal tip by applying electric field
Homma, Yoshikazu	12	Japanese Journal of Applied Physics Part 2-Letters & Express Letters	2007	Reaction products of Co catalysts in ethanol-chemical-vapor-deposition ambient at low-pressure studied by in situ X-ray photoelectron spectroscopy
Homma, Yoshikazu	13	Nano Letters	2007	Carbon nanotube growth from semiconductor nanoparticles
Homma, Yoshikazu	14	Chemical Physics Letters	2007	Gold-filled apo-ferritin for investigation of single-walled carbon nanotube growth on substrate
Homma, Yoshikazu	15	Chemical Physics Letters	2007	Direct observation of single-walled carbon nanotube growth processes on SiO_2 substrate by in situ scanning electron microscopy
Homma, Yoshikazu	16	Applied Physics Express	2008	Growth of single-walled carbon nanotubes from ceramic particles by alcohol chemical vapor deposition
Homma, Yoshikazu	17	Japanese Journal of Applied Physics	2008	Effect of ambient gas on the catalytic properties of Au in single-walled carbon nanotube growth
Homma, Yoshikazu	18	Japanese Journal of Applied Physics	2008	Growth of vertically aligned single-walled carbon nanotubes on alumina and sapphire substrates
Homma, Yoshikazu	19	Nano Letters	2008	Mechanism of gold-catalyzed carbon material growth
Homma, Yoshikazu	19	Nano Letters	2008	Mechanism of gold-catalyzed carbon material growth
Homma, Yoshikazu	20	Nano Letters	2008	Atomic-scale in-situ observation of carbon nanotube growth from solid state iron carbide nanoparticles
Homma, Yoshikazu	21	Nano Research	2009	Single-Walled Carbon Nanotube Growth with Non-Iron-Group "Catalysts" by Chemical Vapor Deposition
Homma, Yoshikazu	22	Reports on Progress in Physics	2009	Suspended single-wall carbon nanotubes: synthesis and optical properties
Homma, Yoshikazu	23	Nanotechnology	2009	The controlled growth of horizontally aligned single-walled carbon nanotube arrays by a gas flow process
Homma, Yoshikazu	24	Nano Letters	2009	Atomic-Scale Analysis on the Role of Molybdenum in Iron-Catalyzed Carbon Nanotube Growth
Homma, Yoshikazu	25	Applied Physics Express	2010	Vertical Sheet Array of Carbon Nanotubes Grown on Sapphire Substrates Using Atomic Step Distribution
Homma, Yoshikazu	26	Journal of Physical Chemistry C	2012	Comparative Study of Catalytic Activity of Iron and Cobalt for Growing Carbon Nanotubes on Alumina and Silicon Oxide
Homma, Yoshikazu	27	Materials Express	2012	Vertically-Aligned Carbon Nanotube Growth Using Closely Packed Iron Oxide Nanoparticles
Homma, Yoshikazu	28	Catalysts	2014	Gold Nanoparticles as the Catalyst of Single-Walled Carbon Nanotube Synthesis
Homma, Yoshikazu	29	Applied Physics Letters	2014	Structurally inhomogeneous nanoparticulate catalysts in cobalt-catalyzed carbon nanotube growth
Homma, Yoshikazu	30	Japanese Journal of Applied Physics	2015	Thermal behavior of metal layers sandwiched by silicon dioxide layers
Homma, Yoshikazu	31	Carbon	2015	Re-growth of single-walled carbon nanotube by hot-wall and cold-wall chemical vapor deposition
Milne, WI at University of Cambridge	1	Journal of Vacuum Science & Technology B	2002	Characteristics of multiwalled carbon nanotube nanobridges fabricated by poly(methylmethacrylate) suspended dispersion
Milne, WI at University of Cambridge	2	Microelectronic Engineering	2002	Study of multi-walled carbon nanotube structures fabricated by PMMA suspended dispersion
Milne, WI at University of Cambridge	3	Nanotechnology	2002	Fabrication and electrical characteristics of carbon nanotube field emission microcathodes with an integrated gate electrode
Milne, WI at University of Cambridge	4	Nano Letters	2003	Superhydrophobic carbon nanotube forests
Milne, WI at University of Cambridge	5	Journal of Vacuum Science & Technology B	2003	Fabrication of multiwalled carbon nanotube bridges by poly-methylmethacrylate suspended dispersion
Milne, WI at University of Cambridge	6	Journal of the Mechanics and Physics of Solids	2003	Determination of mechanical properties of carbon nanotubes and vertically aligned carbon nanotube forests using nanoindentation
Milne, WI at University of Cambridge	7	Microelectronic Engineering	2003	Lateral field emitters fabricated using carbon nanotubes
Milne, WI at University of Cambridge	8	Nano Letters	2004	Self-aligned, gated arrays of individual nanotube and nanowire emitters
Milne, WI at University of Cambridge	9	Journal of Materials Chemistry	2004	Carbon nanotubes as field emission sources
Milne, WI at University of Cambridge	10	Nano Letters	2004	The significance of plasma heating in carbon nanotube and nanofiber growth
Milne, WI at University of Cambridge	11	Pure and Applied Chemistry	2006	Carbon nanotubes by plasma-enhanced chemical vapor deposition
Milne, WI at University of Cambridge	12	Nanotechnology	2007	SWCNT growth on Al/Fe/Mo investigated by in situ mass spectroscopy
Milne, WI at University of Cambridge	13	Nanotechnology	2008	Carbon nanotube based photocathodes
Milne, WI at University of Cambridge	14	Nanophotonics Ii	2008	Patterned multiwall carbon nanotube electrode arrays for liquid crystal photonic devices
Milne, WI at University of Cambridge	15	Advanced Materials	2008	Sparse multiwall carbon nanotube electrode arrays for liquid-crystal photonic devices
Milne, WI at University of Cambridge	16	Carbon Nanotubes and Associated Devices	2008	Sparse multiwall carbon nanotube electrodes arrays for liquid crystal photonic devices
Milne, WI at University of Cambridge	17	Liquid Crystal Xii	2008	Sparse multiwall carbon nanotube electrodes arrays for liquid crystal photonic devices
Milne, WI at University of Cambridge	18	Carbon	2009	Efficient diffusion barrier layers for the catalytic growth of carbon nanotubes on copper substrates
Milne, WI at University of Cambridge	19	Nanotechnology	2009	Carbon nanotubes integrated in electrically insulated channels for lab-on-a-chip applications
Milne, WI at University of Cambridge	20	Journal of Physical Chemistry C	2009	Acetylene: A Key Growth Precursor for Single-Walled Carbon Nanotube Forests

	Paper Number	Journal	year	Title
Milne, WI at University of Cambridge	21	Nano Letters	2011	High Throughput Nanofabrication of Silicon Nanowire and Carbon Nanotube Tips on AFM Probes by Stencil-Deposited Catalysts
Milne, WI at University of Cambridge	22	Journal of Micromechanics and Microengineering	2011	Vertically aligned CNT growth on a microfabricated silicon heater with integrated temperature control-determination of the activation energy from a continuous thermal gradient
Milne, WI at University of Cambridge	23	Carbon	2011	The mechanism of the sudden termination of carbon nanotube supergrowth
Milne, WI at University of Cambridge	24	Advances in Nanodevices and Nanofabrication	2012	Novel Nanostructured Carbon Nanotube Electron Sources
Milne, WI at University of Cambridge	25	Acs Nano	2012	Hot Electron Field Emission via Individually Transistor-Ballasted Carbon Nanotube Arrays
Milne, WI at University of Cambridge	26	Sensors	2012	A Critical Review of Glucose Biosensors Based on Carbon Nanomaterials: Carbon Nanotubes and Graphene
Milne, WI at University of Cambridge	27	Materials	2013	Plasma Enhanced Chemical Vapour Deposition of Horizontally Aligned Carbon Nanotubes
Milne, WI at University of Cambridge	28	Applied Physics Letters	2014	Field emission properties from flexible field emitters using carbon nanotube film
Milne, WI at University of Cambridge	29	Emerging Nanotechnologies for Manufacturing, 2nd Edition	2015	Engineered carbon nanotube field emission devices
Ajayan, PM at Rice	1	Applied Physics Letters	2000	Lift-up growth of aligned carbon nanotube patterns
Ajayan, PM at Rice	2	Journal of Nanoscience and Nanotechnology	2001	Carbon nanotube-magnesium oxide cube networks
Ajayan, PM at Rice	3	Science and Technology of Nanostructured Materials	2001	Tailoring carbon nanotube growth
Ajayan, PM at Rice	4	Applied Physics Letters	2002	Growth of aligned carbon nanotubes on self-similar macroscopic templates
Ajayan, PM at Rice	5	Materials Science & Engineering C-Biomimetic and Supramolecular Systems	2002	Carbon nanotube network growth on palladium seeds
Ajayan, PM at Rice	6	Nano Letters	2002	Structural characterizations of long single-walled carbon nanotube strands
Ajayan, PM at Rice	7	Journal of Physical Chemistry B	2003	Role of transition metal catalysts in single-walled carbon nanotube growth in chemical vapor deposition
Ajayan, PM at Rice	8	Journal of Physical Chemistry B	2003	High-density, large-area single-walled carbon nanotube networks on nanoscale patterned substrates
Ajayan, PM at Rice	9	Composites Science and Technology	2003	Multifunctional structural reinforcement featuring carbon nanotube films
Ajayan, PM at Rice	10	Chemistry of Materials	2003	Assembly of highly organized carbon nanotube architectures by chemical vapor deposition
Ajayan, PM at Rice	11	Journal of Applied Physics	2005	Anisotropic thermal diffusivity of aligned multiwall carbon nanotube arrays
Ajayan, PM at Rice	12	Journal of Nanoscience and Nanotechnology	2005	Flow-induced planar assembly of parallel carbon nanotubes and crossed nanotube junctions
Ajayan, PM at Rice	13	Applied Physics Letters	2006	Contact transfer of aligned carbon nanotube arrays onto conducting substrates
Ajayan, PM at Rice	14	Applied Physics Letters	2006	Multisegmented one-dimensional hybrid structures of carbon nanotubes and metal nanowires
Ajayan, PM at Rice	15	Journal of Nanoscience and Nanotechnology	2007	Anisotropic thermal diffusivity characterization of aligned carbon nanotube-polymer composites
Ajayan, PM at Rice	16	Advanced Materials	2007	Ultrathick freestanding aligned carbon nanotube films
Ajayan, PM at Rice	17	Journal of Physical Chemistry C	2007	The role of dislocations at the catalyst-wall interface in carbon nanotube growth
Ajayan, PM at Rice	18	Carbon	2007	Densified aligned carbon nanotube films via vapor phase infiltration of carbon
Ajayan, PM at Rice	19	Journal of Physical Chemistry C	2008	Controlled CCVD synthesis of robust multiwalled carbon nanotube films
Ajayan, PM at Rice	20	Nanotechnology	2008	Air-assisted growth of ultra-long carbon nanotube bundles
Ajayan, PM at Rice	21	Nanotechnology	2008	Time and temperature dependence of multi-walled carbon nanotube growth on Inconel 600
Ajayan, PM at Rice	22	Nanotechnology	2009	Passivation oxide controlled selective carbon nanotube growth on metal substrates
Ajayan, PM at Rice	23	Journal of Nanoscience and Nanotechnology	2010	Modifying Surface Structure to Tune Surface Properties of Vertically Aligned Carbon Nanotube Films
Ajayan, PM at Rice	24	Scientific Reports	2012	Covalently bonded three-dimensional carbon nanotube solids via boron induced nanojunctions
Ajayan, PM at Rice	25	Composites Science and Technology	2012	Application of continuously-monitored single fiber fragmentation tests to carbon nanotube/carbon microfiber hybrid composites
Ajayan, PM at Rice	26	Chemical Physics Letters	2013	Thin micropatterned multi-walled carbon nanotube films for electrodes
Ajayan, PM at Rice	27	Acs Nano	2013	Three-Dimensional Metal-Graphene-Nanotube Multifunctional Hybrid Materials
Ajayan, PM at Rice	28	Acs Applied Materials & Interfaces	2014	Enhanced Field Emission Properties from CNT Arrays Synthesized on Inconel Superalloy